Sustainable Cities and Society 143 (2026) 107357

Contents lists available at ScienceDirect

Sustainable Cities and Society

journal homepage: www.elsevier.com/locate/scs

The influence of urban geometry and vegetation on summer thermal comfort: an integrated methodology to assess microclimate variations across Local Climate Zones

Anna Codemo *, Gianluca Maracchini, Sara Favargiotti, Rossano Albatici

Department of Civil Environmental Mechanical Engineering, University of Trento, Italy

ARTICLE INFO

Keywords:
Local climate zones
Microclimate modelling
Outdoor thermal comfort
UWG
ENVI-met
Climate-sensitive urban planning

ABSTRACT

Urban areas are unprecedentedly under pressure due to global warming, heatwaves and the urban heat island effect. As thermal stress increases, the evaluation of thermal comfort across the city is crucial to design climate resilient spaces. However, few studies investigate microclimate variations across several areas in the city to understand the influence of geometry and vegetation. This study investigates the role of urban geometry and vegetation in improving pedestrian thermal comfort in Trento, an alpine city in north-eastern Italy. Four neighbourhoods identified by different Local Climate Zones are selected for the analysis. To determine summer outdoor thermal comfort, microclimate parameters and the physiologically equivalent temperature (PET) are calculated through a workflow combining the Urban Weather Generator (UWG) tool and ENVI-met considering the existing spatial configuration of the neighbourhoods in present and future projected climatic contexts. A 24-hour simulation is performed for a hot day and validated through micrometeorological measurements conducted in July 2024. The results show the variations in thermal stress between LCZs and within the areas. While compact areas show higher temperatures during the night, during daytime they have lower values of thermal stress due to shade. Shade provided by geometry seems to have more influence than the effect of vegetation in improving comfort. The proposed workflow starting from a single climate dataset processed with UWG to represent the study areas facilitates the assessment of multiple areas. The results contribute to a better understanding of microclimates in urban areas and of the impact of climate change, vegetation and geometry on heat stress.

1. Introduction

In the last decades, urban areas have been causing increasing concerns due to the negative impact of rapid urbanisation on urban liveability and citizens' well-being (Chatzipoulka et al., 2020; Chen et al., 2022; Lee et al., 2018). As almost two-thirds of the global population resides in urban areas, with this share expected to grow in the following years (UN Habitat, 2022), the increased vulnerability of cities to climate-related stressors requires sustainable solutions improving urban conditions (Kleerekoper et al., 2012; Rydin et al., 2012; Wang et al., 2021). Indeed, urban fabric and the expansion of impervious surfaces, such as concrete and asphalt, replacing green areas, create the conditions for the rise of local temperatures (Ouyang et al., 2020). This phenomenon, also known as the Urban Heat Island (UHI) effect, exacerbates the impact of extreme weather events on human health, particularly heatwaves (Oke et al., 2017). It leads to greater reliance on air conditioning to reduce indoor summer overheating, which in turn increases energy consumption, greenhouse gas emissions (Fu et al., 2025; Halkos & Gkampoura, 2021; López-Cabeza et al., 2023; Magli et al., 2015) as well as waste heat contributing to UHI (Shooshtarian et al., 2020). These considerations are particularly relevant in light of the future climate projections. According to the IPCC's Sixth Assessment Report, an increase in global temperature is expected, ranging between 1.1°C and 5.7°C by 2100 (IPCC, 2023). Therefore, rising temperatures, coupled with altered precipitation and humidity levels, will challenge the resilience of urban environments, making adaptive strategies for Outdoor Thermal Comfort (OTC) and energy-efficient cooling even more critical (Kim et al., 2025).

Abbreviations: AT, Air Temperature; H/W, Height-width ratio; LCZ, Local Climate Zone; MRT, Mean Radiant Temperature; OTC, Outdoor Thermal Comfort; PET, Physiological Equivalent Temperature; SVF, Sky View Factor; UWG, Urban Weather Generator.

* Corresponding author.
E-mail address: anna.codemo@unitn.it (A. Codemo).

https://doi.org/10.1016/j.scs.2026.107357
Received 3 October 2025; Received in revised form 15 January 2026; Accepted 31 March 2026
Available online 2 April 2026

Integrating adaptive strategies in the planning and design processes coping with spatial development is an effective strategy to foster human health and wellbeing (Lafortezza et al., 2018). City-level planning indeed plays a crucial role for integrating superordinate legislation and spatializing solutions (Stead & Meijers, 2009). Innovative urban planning approaches can improve urban resilience and reduce health risks, by fostering climate change adaptation measures, also contributing to climate change mitigation — for instance, by reducing cooling energy demands (Grêt-Regamey et al., 2017; Salehi & Nasrollahi, 2024; Song et al., 2020). However, while tools like land use policies and advanced modelling techniques could support these goals, existing urban planning frameworks often fail to account for local microclimates and context-specific solutions (LIU & WU, 2022). Current strategies are indeed generic, introducing broad concepts and not including microclimate optimization (Banerjee et al., 2024). Despite few studies investigate the link between urban planning policies and urban microclimates, current planning practices do not take into consideration the different microclimates within cities and future climate projections (Ebrahimabadi et al., 2015; Heris et al., 2020; Luo et al., 2024; Zhang et al., 2024). Indeed, a lack of integration of cities' climate change policies (Hurlimann et al., 2021) and urban climate knowledge are detected in land-use planning tools and zoning policies (Heris et al., 2020). Starting from this consideration, the present work addresses the challenge to integrate context-based microclimate knowledge into urban planning tools through an integrated assessment methodology.

Urban microclimates show high temporal and spatial variability due to the diverse urban characteristics, such as building geometry, amount of vegetation, land cover, and surface roughness (Lai et al., 2019). These factors interact to create localised microclimates, forming a mosaic of distinct climate zones within cities shaped by the interplay between artificial surfaces and green spaces. Stewart and Oke (2012) defined these variations as Local Climate Zones (LCZs), while in other cases they are referred to as climatopes (Scherer et al., 1999). To provide context-specific policies, more research is needed to compare microclimates in different types of cities and under different conditions (Perera & Emmanuel, 2018; Yang et al., 2019).

1.1. Urban spatial configurations and microclimate variations

Few studies have adopted the LCZs classification to explore its application in terms of OTC (e.g. Geletič et al., 2018; Lam et al., 2023; Lau et al., 2019; Liu et al., 2018; Top et al., 2020). Top et al. (2020), for example, assessed meteorological variables and OTC conditions in various LCZs of Ghent, Belgium, under heat wave conditions using data from local weather stations. Lam et al. (2023) combined meteorological measurements with thermal comfort surveys to identify thermal comfort patterns in LCZs of Melbourne, Australia. However, these studies assess intra-urban variations overlooking the internal variations within each LCZ, limiting the understanding of the impact of urban fabric and vegetation on outdoor microclimate.

For internal variations, OTC studies focus on the impacts on microclimate of the built environment. However, they mainly address one aspect of the built environment, such as urban form and urban canyons (Georgakis & Santamouris, 2006; Maracchini et al., 2022; Middel et al., 2014; Nasrollahi & Rostami, 2023; Taleghani et al., 2015; Othman & Alshboul, 2020), vegetation and green spaces (Bowler et al., 2010; Herath et al., 2024; Morakinyo & Lam, 2016; Motie et al., 2023; Wong et al., 2021; Zhao et al., 2018), or surface material characteristics (Alchapar & Correa, 2016; Erell et al., 2014; Lobaccaro & Acero, 2015; Taleghani & Berardi, 2018). For a complete understanding of real conditions, it would be practical to simultaneously assess more aspects. Furthermore, most of the studies assess thermal comfort under present climate conditions. However, Abedrabboh et al. (2025) and Sola-Caraballo et al. (2024), by assessing OTC under future climate projections in 2050 and 2080, showed that climate sensitive urban transformations should take into account that OTC will be severely affected by the

Table 1
Characteristics of studies that have investigated microclimate variables and human thermal comfort in multiple areas.

Scenarios	Object	Scale	Season	Input meteo	Evaluated variables	Analysis	Model dimension	Resolution	Climate	Location	Reference
SQ+SC	3 areas 4 scenarios	Neighbourhood	Summer	1 weather station outside areas	AT, RH, WS, PET, MRT, surface energy balance	Effect of vegetation	800 × 800m	10m	Cfb	Melbourne, Australia	Herath et al., 2024
SQ	3 areas	Block	Summer and winter	*Not specified*	AT, MRT, PET	Effect of geometry	100 × 100m	3m	BSk	Mashhad, Iran	Darbani et al., 2023
SQ+SC	2 areas 4 scenarios	Neighbourhood	Summer	1 weather station outside areas	Tsurf, Ta, MRT, WS, PET	Cooling effects of scenarios	500 × 500m	3m	Dwb	Suwon City, Korea	Ma et al., 2023
SQ+SC	3 areas 10 scenarios	Block	Summer	1 weather station outside areas	AT, PET, Sensible heat	Tree canopy benefits	175 × 175	2m	Cfa	Nanjing, China	Li et al., 2023
SQ	4 areas	Neighbourhood	Summer	1 weather station outside areas	AT, RH, WS, PET, Building energy consumption	Effect of vegetation	400 × 400m	4m	Dwa	Harbin, China	Dong et al., 2023
SQ+SC	4 areas 10 scenarios	Block	Summer	1 device per area (field measurement used for validation)	PET	Cooling effects of scenarios	< 100 × 100m	1m	Csa	Algeri, Algeria	Arrar et al., 2024
SQ	4 areas 6 scenarios	Block	Winter and summer	*Not specified*	AT, MRT, WS, PET	Effect of orientation Effect of vegetation distribution	< 100 × 100m	*not specified*	Csa	Sanandaj, Iran	Salehi & Nasrollahi, 2024
SQ	6 areas	Block		*Not specified*	AT, MRT, PET	Effect of geometry	250 × 300	*not specified*	Bwh	Ahvaz, Iran	Nasrollahi, 2021
SQ	10 areas	Neighbourhood	Summer	1 weather station outside areas	AT, PET, UTCI	Effect of Local Climate Zone	150 × 150m	1,5m	Aw	Nagpur, India	Kotharkar & Dongarsane, 2024
SQ+SC	2 areas 6 scenarios	Neighbourhood	Summer and winter	1 weather station outside areas	AT, WS, PET,	Effect of aspect ratio Effect of vegetation	240 × 210m	3m	Dwa	Harbin, China	Cui et al., 2023
SQ	2 areas 6 scenarios	Neighbourhood	Summer	1 weather station outside areas	Surface temperature, AT, RH, MRT, PET	Effect of wall materials	400mx300m	4m	Bsh	Shiraz, Iran	Tabatabaei & Fayaz, 2023

increase of temperatures.

Expanding this research to cover diverse urban configurations, climates, and seasons is essential for a comprehensive understanding of microclimatic differences across urban environments (Table 1). Few studies have systematically compared multiple urban areas under consistent settings to explore OTC variations across different areas (Kotharkar & Dongarsane, 2024; Salehi & Nasrollahi, 2024). Kotharkar and Dongarsane (2024) assesses the variation of microclimate parameters and OTC indexes across ten areas identified by LCZs using ENVI-met. Salehi and Nasrollahi (2024) assesses the influence of vegetation on the pedestrian thermal environment in three areas characterized by different urban forms and orientations. However both studies adopted identical boundary conditions for all the areas, overlooking the effect of UHI on the context. This approach seems common in comparative studies. For example, Ma et al. (2023) investigate the impact of project developments in two areas using the same meteorological boundary conditions. Herath et al. (2024) assess the impact of green areas configurations in 3 areas characterized by different LCZs using as boundary conditions data from the closest public weather station. Adopting different boundary conditions reflecting the surrounding urban microclimate is particularly relevant when dealing with studies comparing multiple areas, as they might have daytime and nighttime temperature differences due to UHI (Emery et al., 2021; Leconte et al., 2015; Shi et al., 2018). Some studies, such as the one of Li et al. (2023), adopt different values for boundary conditions using as input the field measurements also adopted for the validation. However, these measures do not represent boundary conditions rather the meteorological data of a specific point. Conversely, the workflow adopted in Detommaso et al. (2021) to deliver the local boundary conditions in a ENVI-met simulation for an area in Catania, can be useful to address this issue.

Over the past decades, extensive studies have performed numerical simulations in European cities (Lam et al., 2021). In Italy, studies have been conducted in oceanic climate (Cfb) (Fiorillo et al., 2023; Gherri et al., 2021), mediterranean climate (Csa) (Gatto et al., 2021; Salata et al., 2016b), humid subtropical climate (Cfa) (Fabbri et al., 2023; Marchi et al., 2023; Piselli et al., 2018). Alpine cities, such as Trento, characterized by distinctive mountain landscapes have not been addressed yet in outdoor thermal comfort studies. However, these regions experience hot summers with significantly increasing temperatures (Tudoroiu et al., 2016) and longer heatwaves (Morlot et al., 2023). Moreover, they are within the most sensible environments for climate change, being exposed to fast and intense changes (Kotlarski et al., 2023; Napoli et al., 2025).

1.2. Aim and research questions

To overcome these research gaps, this study presents a novel workflow to assess thermal comfort in existing neighbourhoods. The integrated methodology encompasses a novel multiscale framework to ensure consistency of input climatological data in multiple areas across cities and provides simultaneous consideration of the impact of urban form and vegetation on microclimate. Specifically, the research analyses and compares microclimate parameters and OTC in present and future scenarios across four areas within the city of Trento, Italy, characterised by different urban morphologies. Four LCZs are investigated with consistent input data for each study area evaluating inter- and intra-area changes.

We aim to understand the effects of different urban parameters on OTC in this context, with particular attention to the effect of greening and urban geometry, in present and future projected climate conditions. For this purpose, the study seeks to address the following research questions:

RQ1. What are the inter- and intra-variations of Outdoor Thermal Comfort within different urban typologies?

RQ2. What is the impact of urban geometry, vegetation and future climate projections on microclimate parameters and comfort?

RQ3. What is an effective workflow for assessing microclimate parameters in multiple areas aiding climate sensitive planning?

This work provides a framework for urban designers and planners to keep in consideration pedestrian comfort during heatwaves in regeneration practices using empirical and numerical methods.

The paper is structured into three main sections. The first describes the employed methodology, introduces the case study and provides the details of simulations and scenarios. The second presents the results of the simulations and proposes a comparison between the study areas, among specific points within the areas, and considering present conditions and future projections. The third discusses the findings, highlighting the effects of urban geometry and vegetation on microclimate and outlining possible future research directions.

2. Materials and methods

2.1. Methodology outline

The methodology adopted in this research is illustrated in Fig. 1 as a flowchart. The case study focuses on Trento, Italy, selected as a representative example of Alpine cities. A coupled multiscale approach is employed to analyse changes in microclimate parameters and OTC. The workflow is structured in the following steps:

- **Phase 1a**: case study selection and preparation of input material

Four types of neighbourhoods are selected to capture the variability in urban forms and microclimates. Geometrical data (collected from field surveys, consultation of the local cadaster and collection of open geo-data) has been prepared with the QGIS software.

Phase 1b: At the district scale, the UWG tool is used to simulate climatological variables for each neighbourhood, starting from rural conditions. The UWG-generated climatological data is validated against fixed weather stations located in each neighbourhood. The results are used as urban boundary conditions for the ENVI-met model.

- **Phase 2**: microclimate simulation of status quo

Numerical models of the selected neighbourhoods were created and simulated considering current climate conditions with the ENVI-met software to compute microclimate variables and thermal comfort indexes. Resulting Air Temperature (AT) and Relative Humidity (RH) were validated through on-site field monitoring.

- **Phase 3**: future weather scenario and scenario without vegetation

Numerical simulations of the geometrical status quo are performed considering future weather data and of the scenarios without vegetation to derive the impact of climate change and the impact of greening on microclimate.

In the following subsections, we outline the required input data and specific methodologies for each step.

2.2. Study area and climatic conditions

Trento is an alpine city located in the northeast of Italy, characterised by a humid subtropical (Cfa) climate according to the Köppen classification. The provincial meteorological service reports that August 2024 experienced higher-than-average temperatures, with a mean temperature of 26.0°C, the second highest on record (historical mean: 22.4°C) (Piazza et al., 2024). Additionally, the city recorded 13 tropical nights (nights with minimum temperatures above 20°C) in August 2024, the second highest count after 1971, which saw 18 tropical nights. A study by Giovannini et al. (2011) also investigated the UHI effect in both summer and winter, showing significant variations, with diurnal maximum intensity reaching 3°C.

The areas for this study have been chosen after a consultation with the Municipality in order to be representatives of the typical typologies

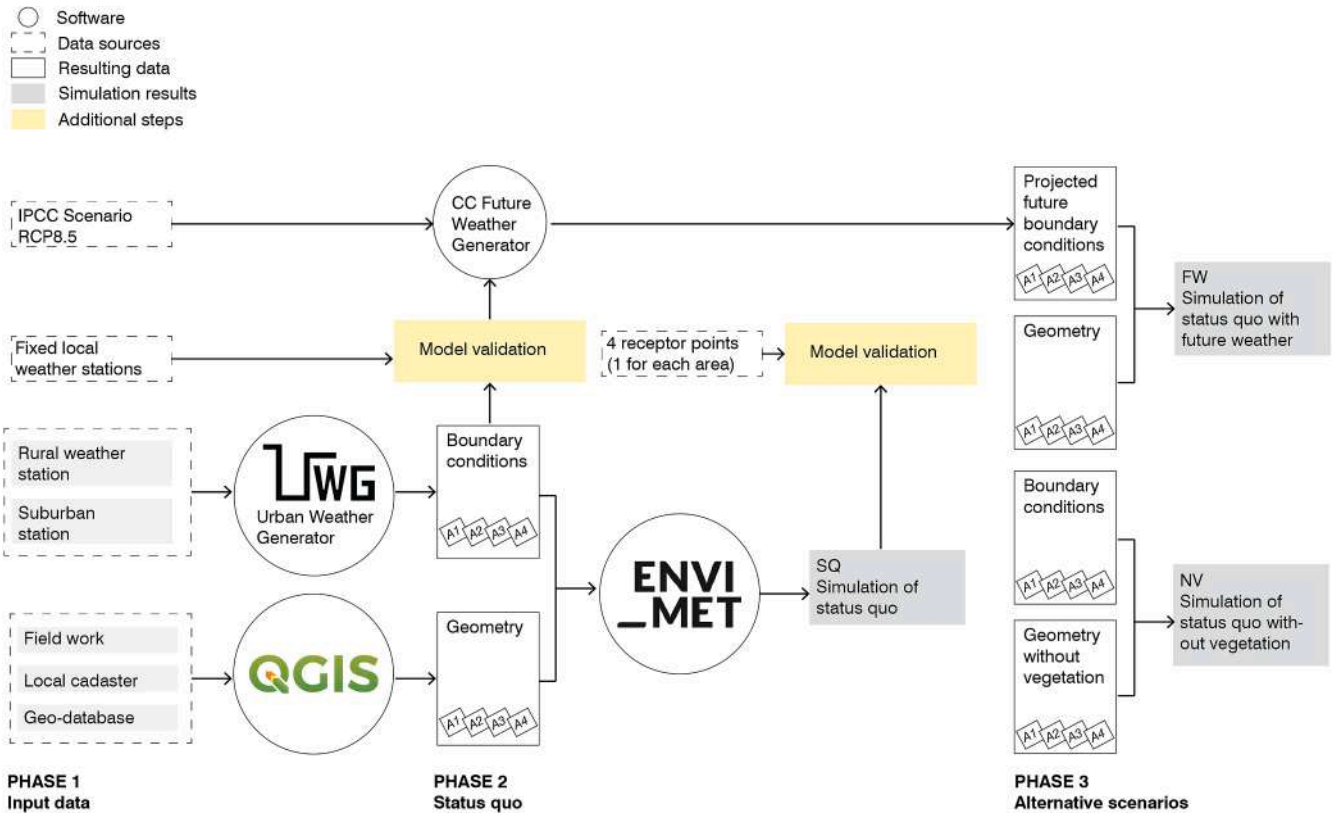

Fig. 1. Workflow of the study: data sources, models adopted, validation processes, analysis and visualisation of results.

present in the city, to be of interest for future retrofitting purposes and to be heterogeneous in their urban morphologies. Specifically, they have

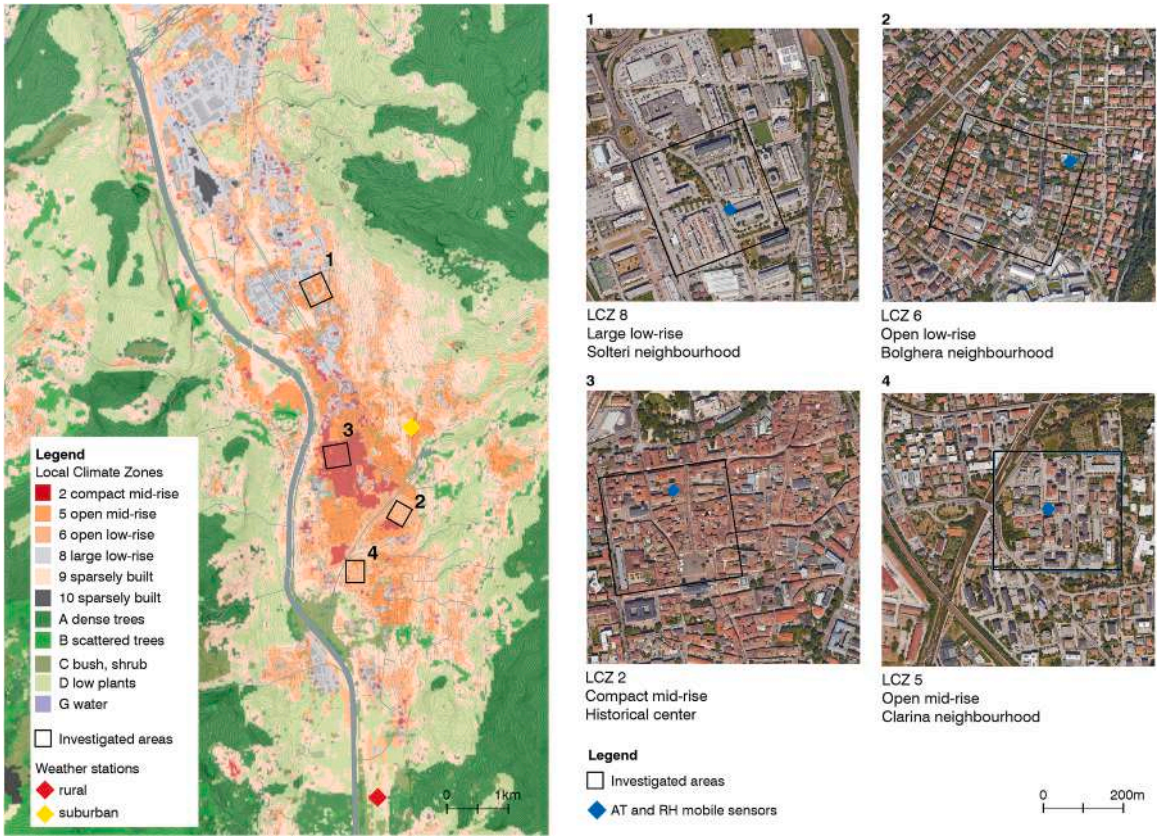

Fig. 2. LCZs classification of Trento, Italy, investigated areas and location of the weather stations.

been selected to represent different Local Climate Zones (LCZ) using the classification (Fig. 2) generated through WUDAPT (Bechtel et al., 2019). This study uses the LCZ map developed by (masked for blind review) produced using SAGA. .

The selected areas represent diverse and common urban forms across the valley floor, useful to investigate the intra-city microclimate variation. These consist of:

- a commercial and residential area (A1) built around 1990 with low-rise buildings and impervious surfaces (LCZ8);
- a residential neighbourhood (A2) built mainly in the first half of 1900 with low rise dwellings with gardens (LCZ6);
- the historical centre (A3), characterised by dense, six-story buildings with limited vegetation (LCZ2);
- a residential district (A4) built mainly between 1960 and 1990 with dense six-story buildings with sparse greenery (LCZ5).

2.3. UWG models configuration

In this study, the UWG simulation tool - Python implementation, version 5.8.0 (Mackey et al., 2020) - was employed to estimate four different hourly AT profiles within the urban canopy layer (one for each selected area) to be used as boundary conditions of the ENVI-met simulations. UWG is a well-established modeling framework for assessing urban microclimate conditions and has been validated in multiple international contexts, including Abu Dhabi (UAE), Toulouse (France), Basel (Switzerland), Singapore, Rome (Italy), and Barcelona (Spain) (Mao et al., 2017), ensuring its robustness and applicability to a wide range of climatic and urban morphologies.

The UWG model integrates four dynamically interacting sub-models, each conceptualized as a distinct node in the system:

- Rural Station Model (RSM) – simulates meteorological conditions in a nearby rural reference site;
- Vertical Diffusion Model (VDM) – calculates the vertical transport of heat and momentum through the atmospheric column;
- Urban Boundary Layer (UBL) – represents the urban-influenced portion of the lower atmosphere;
- Urban Canopy and Building Energy Model (UC-BEM) – captures heat flux exchanges and computes the average air temperature and humidity within the urban canyon.

These components work in tandem to produce a consistent temperature profile, enabling estimation of the thermal impact of urban form and land use, morphing collected environmental variables from a rural station. The model requires as input both meteorological data from a rural weather station—typically assumed to represent the background climate unaffected by urbanization—and aggregated urban morphological and material characteristics of the neighborhood under study, such as surface albedo, vegetation fraction, building heights and thermal properties, as well as traffic data, building HVAC typology and use conditions. The main parameters of the model created for each area are reported in Table 2.

In this work, data from the rural weather station at Trento Airport was used to initialise the model, while mobile sensors placed in each study area were used for preliminary validation (Fig. 2). Fig. 3

2.4. ENVI-met model configuration and scenarios

To investigate microclimate parameters in different urban areas, the simulation tool ENVI-met V5 was employed. ENVI-met is a CFD-based 3D microclimate simulation software that models heat and moisture transfer between building materials, soil surfaces, vegetation, and the atmosphere (Simon et al., 2018). The reliability and accuracy of ENVI-met have been proved by several studies simulating the thermal effects of vegetation, buildings, and streets in many cities (Salata et al., 2016a) and comparing scenarios scenarios (e.g. Lobaccaro & Acero, 2015; Semeraro et al., 2023; Tseliou et al., 2022; Zölch et al., 2016). The areas' input files for ENVI-met 5.6.0 were created using QGIS, incorporating data about surface materials, vegetation, location, and building information. Table 3 summarises the sources for each type of data. For each area, a model measuring approximately 300 m x 300 m was developed, based on field survey data and information from public

Table 2
UWG model parameters for the four chosen areas. Not reported parameters are assumed with default values.

Variable	Description	A1	A2	A3	A4
Rural characteristics					
rurvegcover	Rural vegetation coverage	0.75	0.9	0.9	0.9
h_wind	Wind measurement height [m]	9	100	9	9
Urban morphology and characteristics					
charlength	Urban characteristic length [m]	368	289	363	282.5
blddensity	Building footprint density (urban area fraction)	0.23	0.25	0.54	0.27
bldheight	Average building height [meter]	17.06	11.65	17.06	11.52
vertohor	Vertical to horizontal area ratio	0.62	0.83	1.23	0.72
droad	Thickness of urban road pavement [m]	0.13	0.13	0.06	0.2
croad	Road pavement volumetric heat capacity [J/m^{3}K]	2,140000	2,140000	2,060000	2,120000
kroad	Road pavement conductivity [W/mK]	1.38	1.38	1.54	1.43
albroad	Urban road albedo	0.12	0.12	0.12	0.12
grasscover	Fraction of urban area covered by grass	0.19	0.27	0	0.18
treecover	Fraction of urban ground covered in trees	0.08	0.16	0	0.08
sensanth	Street level anthropogenic heat [W/m^2]	25	10	5	15
schtraffic	Hourly traffic schedule (weekdays, Saturday, Sunday)	[[0.15, 0.06, 0.04, 0.03, 0.02, 0.01, 0.26, 0.64, 0.91, 0.8, 0.64, 0.55, 0.5, 0.5, 0.5, 0.56, 0.74, 0.81, 0.85, 0.68, 0.4, 0.24, 0.22, 0.24], [0.26, 0.13, 0.06, 0.04, 0.02, 0.02, 0.02, 0.09, 0.17, 0.28, 0.38, 0.45, 0.47, 0.38, 0.3, 0.32, 0.38, 0.47, 0.49, 0.51, 0.43, 0.3, 0.28, 0.36], [0.34, 0.19, 0.11, 0.06, 0.02, 0.02, 0.02, 0.04, 0.13, 0.21, 0.3, 0.36, 0.36, 0.3, 0.26, 0.3, 0.38, 0.47, 0.43, 0.38, 0.3, 0.21, 0.17, 0.19]]			
h_mix	Fraction of HVAC waste heat released to street canyon	0.5	1	0	0
Building characteristics					
bld	Matrix representing a fraction of the urban building stock. Class numbers represent building archetypes according to (Carnieletto et al. (2021); Susca et al. (2023))	Class V: 0.15, Class VI: 0.3, Class VII: 0.55	Class III+IV: 0.29, Class VII: 0.33, Class VIII: 0.08, Class IX: 0.15, ClasseX: 0.15	Class I: 1	Class III+IV: 0.17, Class V: 0.28, Class VI: 0.09, Class VII: 0.07, Class VIII: 0.08, Class X: 0.31

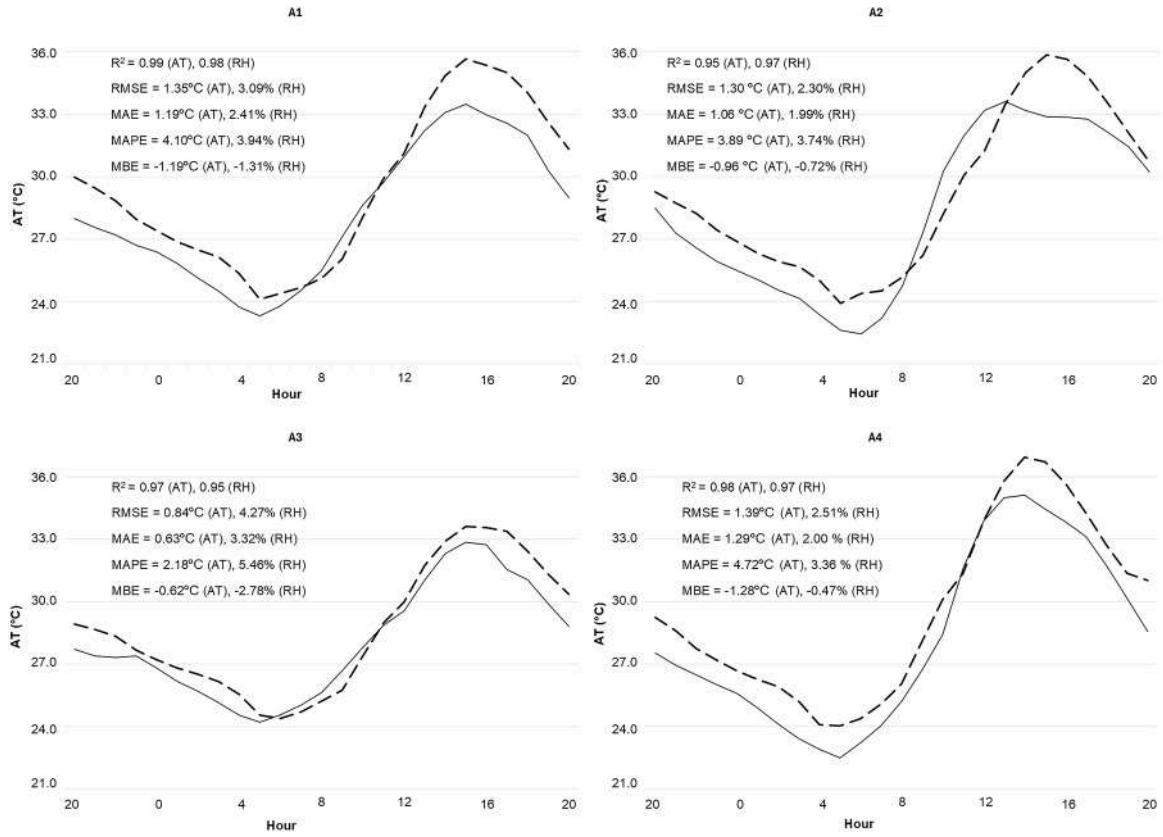

Fig. 3. Validation of AT in the four areas by comparing on-site measurements and simulation results in the receptor points.

Table 3
Sources of data for the ENVI-met models.

	Parameter	Source
Buildings	Shape	Local cadastre
	Height	Local cadastre, Digital Elevation Model
	Materials	Typical classes by construction year according to (Carnieletto et al. (2021); Susca et al. (2023)). Construction and energy refurbishment years have been gathered by the Archive Department of the Municipality of Trento
Trees	Height	Digital Elevation Model, local vegetation cadastre
	Species and genus	Local vegetation cadastre, field survey
Artificial surfaces	Shape	Aerial images, Land use land cover map
	Material	Aerial images, field survey
Pervious surfaces	Shape	Aerial images, Land use land cover map
	Material	Aerial images, field survey

databases. The models' dimensions are slightly different, as made in Herath et al. (2024), as the borders have been designed to avoid cutting buildings and to pass through the middle of streets.

Roof and external wall characteristics were defined using materials from the ENVI-met database. Classes of buildings' construction ages were identified through the database provided by the Municipality, and associated with the typical materials adopted in Italy by construction age classes derived by the inventories of Carnieletto et al. (2021) and Susca et al. (2023). Walls' and roofs' stratigraphies were then accordingly created on the ENVI-met database. For pervious and impervious surfaces, materials from the same database were considered. For the vegetation input, approximately 50 species found across the four areas were identified and mapped using the ENVI-met built-in Albero database. Consistent with previous studies (Liu et al., 2021; Dong et al., 2023), we used morphological parameters such as height, trunk height, foliage density and crown diameter to represent each tree species in the numerical simulations. Starting from the local tree cadaster and field visits, we defined tree species and geometry. The most common species in these areas are birch, hornbeam, maple, plum, oak, lime, elm, spruce, covering in different percentages the trees' categories. To model each tree, we used the built-in library in Albero, modifying geometrical characteristics if needed. Other characteristics, such as basic plan physiology, were not modified from the library. Further details are available in Table A.1. The geometry of the simulation model is outlined in Table 4.

Meteorological boundary conditions were used as full-forcing inputs

Table 4
Overview of physical and geometrical properties of the four investigated areas.

	A1	A2	A3	A4
Latitude and longitude	46.091425, 11.117685	46.059240, 11.132066	46.068518, 11.121292	46.052584, 11.124236
Altitude (m asl)	191	206	193	196
Model domain (m)	332 × 361 × 82	306 × 272 × 82	406 × 220 × 82	270 × 296 × 82
Model resolution (m)	2	2	2	2
Total area of site (m^2)	120131	83116	130232	79904
Mean height of the blocks (m)	17.8	11.6	16	11.5
Number of nesting grids	8	6	7	6
Telescoping factor	20	20	20	20

to initialise the ENVI-met model, using the outputs of the UWG model. AT and RH, provided by the UWG model, are specific for each investigated area. Solar radiation (hourly global, direct and diffuse solar radiation data) is collected from an urban meteorological station characterized by the same solar exposure of the selected areas. Wind speed and direction is kept constant (2m/s and 235°) to guarantee model stability (Alsaad et al., 2022). The prevailing wind direction is south-west (235°) with a speed of 2m/s. The detailed weather data and wind profiles are presented in Fig. A.1. The simulation ran for 48 hours, with the first 24 hours excluded to avoid simulation errors. Table 5 summarises the main characteristics of the simulation. OTC metrics were generated using Bio-met 5.6.0, which calculates the Physiological Equivalent Temperature (PET) based on personal human parameters, following the guidelines of ISO 7730 (ISO, 2005) and ASHRAE-2010 (ASHRAE, 2010).

To accomplish this investigation, the following scenarios have been investigated in the four selected areas:

- *Base model (SQ)*: status quo of the site carefully selecting all existing conditions.
- *No-vegetation model (NV)*: all existing vegetation (trees and grass) is removed to determine the impact of greening by comparing the simulations with and without vegetation.
- *Future weather model (FW)*: the model with existing geometry is simulated with future climate conditions using the RCP8.5 climate projection from the IPCC for 2050, determined through ccWeatherGenerator (Jentsch et al., 2012). The Climate Change World Weather Generator is an open access tool previously used by several studies (P.Tootkaboni et al., 2021; Sola-Caraballo et al., 2024) morphing experimental data with future weather projections. The RCP8.5 scenario, used in previous studies (Ascione et al. 2024; Tsoka et al., 2025), has been selected to represent the worst predictions presented by the IPCC based on HadCM3. These scenarios are established by the major global authorities and are officially recognized by administrators. The comparison between the simulation results with present and future climate determines the impact of climate change.

2.5. Model validation

To ensure robustness of results, thermal outputs of the ENVI-met simulations of the SQ are validated by comparing the results of the simulations with in-situ measurements in a receptor point. Four mobile temperature and humidity sensors (Lascar Electronics, EasyLog EL-SIE-2+), equipped with solar shields, were used to validate the ENVI-met model results. The sensors have an AT range of −18 to +55°C (precision ±0.2°C) and a relative humidity range of 0 to 100% (precision ±1.5%) recording with 10 minutes frequency. Meteorological data were collected simultaneously across the selected areas on typical hot summer days, over seven consecutive days (168 hours) at the end of July 2024. Numerical values of AT and RH of the SQ scenario were compared with the observed values from the field monitoring at 60-minute intervals. Five statistical metrics were adopted for the model evaluation: coefficient of determination (R^2), root mean square error (RMSE), mean absolute error (MAE), mean absolute percentage error (MAPE), and mean bias error (MBE) (Moriasi et al., 2007).

Table 5
ENVI-met model set up and meteorological input data for the study simulation runs.

Parameters	Values
Start date	July 26, 2024
Start time	00:00
Simulation time	48 hours
Wind speed (average)	2 m/s
Wind direction (average)	235°
Roughness length	0.1
Building initial temperature	25°C

2.6. Analysed parameters

Using the ENVI-met simulations' results, we calculated AT, RH, MRT, and PET for each area over a 24-hour period. Heat maps and variation maps were created for each area at daytime and nighttime to highlight spatial variations and identify key areas. Thermal comfort at the pedestrian level was assessed with PET, as it is widely used in microclimate studies (Liu et al., 2021). In the context of the study, high PET values (>41 °C) represent "very hot" thermal sensation, medium PET values (18–23 °C) indicate "comfortable" conditions (Matzarakis et al., 1999).

The four investigated areas were assessed in different ways: a) comparing hourly mean values across the four areas to assess differences between LCZs; b) assessing the impact of the height-to-width (H/W) ratio and vegetation, and c) comparing the mean values of each area across different time spans to evaluate the effect of climate change.

3. Results

3.1. ENVI-met model validation

Hourly meteorological records of AT and RH from July 26-27 2024 were compared with the corresponding modelled values in four receptors, one per each area. The curves of simulated and measured AT in the four areas are presented in Fig. 4 and show a good fit, with simulated values slightly exceeding measured data in the hottest hours. The metrics were found to be within acceptable ranges (Detommaso et al., 2021; Herath et al., 2024; Ouyang et al., 2022; Salata et al., 2016a), confirming that the ENVI-met model is validated and provides reasonable predictions.

Considering the results of each area, for AT, R^2 achieved values above 0.95. RMSE showed values between 1.39°C and 0.84°C. The MAE obtained values are between 1.29°C and 0.63°C. MAPE resulted between 4.72°C and 2.18°C. MBE showed that values were generally overestimated (−1.28°C and −0.62°C). Similar differences have occurred in previous studies validating one receptor point (e.g Lai et al., 2023; Li et al., 2023; Nasrollahi et al., 2021).

3.2. Comparison between the four neighbourhoods

A comparative analysis of daytime and night-time assessment of AT, MRT and PET has been carried out to evaluate possible variations between and within the four areas. The simulation results in terms of AT at the height of 1.8 m in the four neighbourhoods are reported in Fig. 4 as boxplots, showing the extent of variation within the area and between areas. The results show that A1 is the hottest area at 12:00, 16:00 and 20:00, while A3 (historical centre) is the hottest at 00:00, 04:00 and 08:00.

The assessment of AT and MRT during diurnal and nocturnal periods reveals variations across the study areas. These variations attain their maximum significance during the warmest hours of the day (15:00-17:00). Specifically, A1 exhibits higher mean values of AT and MRT, while the A2 and A3 areas demonstrate lower values during the warmest hours. As illustrated in Fig. 5, the mean values of AT, MRT and PET across the four areas for 24 hours show significant variations. A1 (LCZ8) and A4 (LCZ5) experience the highest values of AT, MRT and PET during the warmest hours of the day. A2 (LCZ6) shows extreme values during daytime, but significant lower values of AT and MRT compared to the previous areas. Conversely, A3 (LCZ2) observed significant differences with the previous areas during daytime in terms of AT, MRT and PET. During nighttime, the pattern is different, and the variations between areas are lower. The highest values of AT and PET are exhibited by A3, followed by A1, A2 and A4 which do not present significant variations.

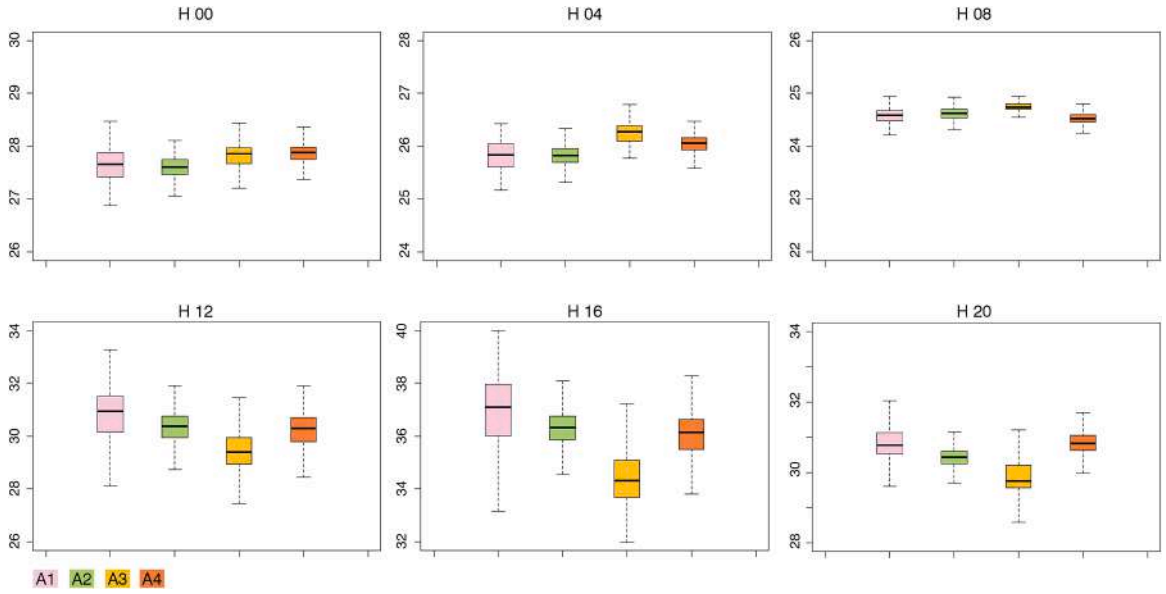

Fig. 4. Boxplot of AT values occurring in the four investigated areas at specific hours.

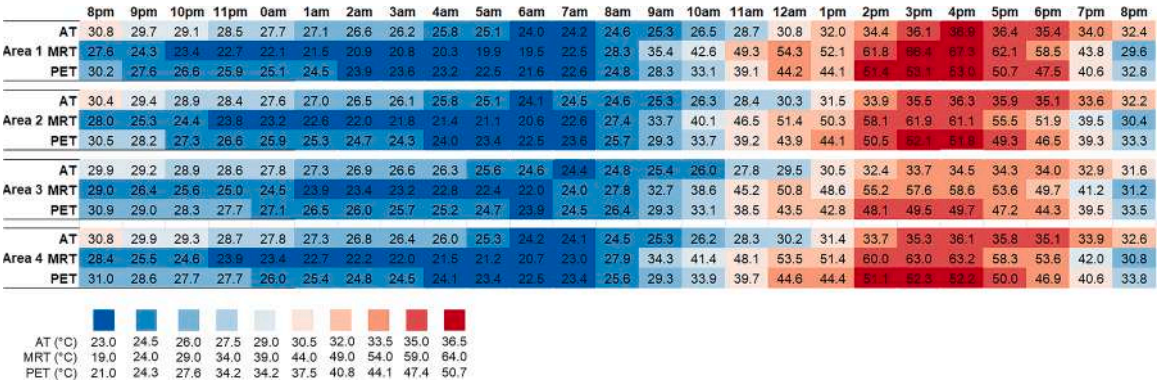

Fig. 5. Daily mean values of AT, MRT, and PET across the four investigated areas.

As shown in Fig. 6, the mean values of PET at 20:00 are comparable across the areas, ranging between 30°C and 31°C, while all points vary between 26°C and 57°C. At 00:00, the differences between the areas increase, with A1 and A2 around 25°C, A4 at 26°C and A3 at 27°C. This pattern is replicated at 04:00, with the urban heat island effect (A3) evident. At 08:00, mean PET is around 25°C in all four areas, indicating slight heat stress. At 12:00, mean conditions are of high thermal stress, with the historical centre having slightly better conditions than the other areas. At 16:00, the areas exhibit the most unfavourable PET values, with the historical centre registering approximately 2°C lower than the other areas. The presence of both vegetation and buildings provides shade to these areas, thereby reducing MRT and enhancing thermal comfort during the diurnal period. Conversely, during nocturnal hours, denser areas demonstrate the poorest performance.

3.3. Microclimate conditions and urban fabric

Significant variations across all LCZs were evident during peak daytime hours. As the chosen simulation day was one of the hottest days of the year, the simulated data for the existing situation display overall hot and very hot conditions. Areas with lower heat loads are found only in the shadow of buildings and trees. To further study the variability of thermal comfort predictors in the area, receptor points are selected for comparing the simulation results. These receptor points were chosen in order to compare streets with different orientations and H/W values, showing the effect of urban geometry on thermal comfort (Table 6, Fig. A.2).

3.3.1. Commercial neighbourhood (A1)

The highest values of AT occur in the two E-W oriented streets (see e.g. P1 and P3, Fig. 7a). High values occur in the parking lots, which are mainly paved and not shaded by trees. The lower values occur in the green area and in the north-exposed areas next to the buildings. The highest PET values in area A1 are observed in the parking zones adjacent to buildings, while the lowest values are found in shaded locations. Vegetation has the most noticeable impact on PET in large, tree-shaded green spaces, as opposed to smaller green areas. Along the streets, vegetation-related cooling is more pronounced on those oriented north-south.

As visible in Fig. 7b, during the coldest hours, P1 has the highest PET values, with a difference of around 4°C with P2 and P4. During these hours the points present a difference of AT between 0.5°C and 1°C and a significant WS difference (P1 is around 0.25 m/s while P2 and P4 are around 1.65m/s). Moreover, there is a difference of around 3% in terms of RH.

During the daytime, P1 has a consistently higher PET value than the other three points, especially between 13:00 and 14:00, when it is 4°C higher than P2 and P4, and 12°C higher than P3. P3 has significantly lower PET values between 14:00 and 15:00 due to the shadow effect. Between 14:00 and 18:00, P1 becomes the point with the lowest PET

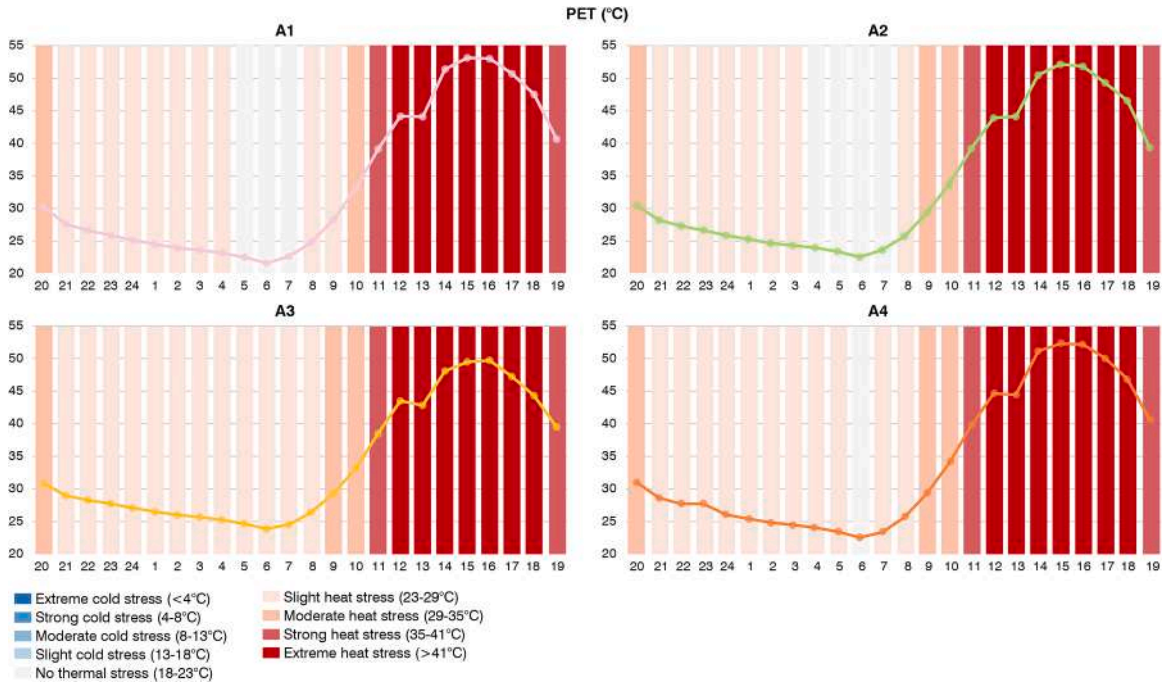

Fig. 6. Daily PET values and thermal sensation ranges across the four investigated areas.

Table 6
H/W values and orientation of the receptor points in the four selected areas.

	A1				A2				A3				A4			
	P1	P2	P3	P4	P1	P2	P3	P4	P1	P2	P3	P4	P1	P2	P3	P4
H/W	0.68	0.62	0.68	0.46	1.31	0.45	0.72	0.91	2.13	1.23	3	1.68	1.21	0.68	0.46	0.96
Orientation	NW	NE	NW	NE	NE	NW	NE	NW	NW	N	NE	NE	N	N	E	E

values as it is in the shade.

3.3.2. Residential neighbourhood (A2)

In A2, the typology characterized by small dwellings with gardens demonstrates the beneficial impact of vegetated gardens on PET values, both during daytime and nighttime. The highest PET values are observed in areas adjacent to streets lacking tree cover and in fully paved zones (Fig. 8a).

At 20:00, 00:00, 04:00, 08:00, AT values are the lowest in the larger green areas. These areas remain cool until early morning, after which the temperature starts to increase. At 12:00 and 16:00, the hottest areas are the streets. During the night, P3 has PET values around 3°C higher than the other points (28°C); indeed, WS is lower than the other values. During the day, PET values are homogeneous in the receptor points, except between 13:00 and 17:00 due to the shadow effect (Fig. 8b).

3.3.3. Historical center (A3)

In the historical center, the highest PET values are recorded in paved open spaces such as squares and large courtyards. In contrast, small courtyards exhibit the lowest levels of heat stress due to their limited exposure to solar radiation (Fig. 9a). At 16:00, PET values indicate moderate heat stress (29.1–35 °C) in small courtyards, strong heat stress (35.1–41 °C) in north-south oriented streets, and extreme heat stress (above 41 °C) in squares. As the historical center contains few trees, shading effects are primarily related to buildings. The difference between maximum and minimum PET values in shaded areas reaches approximately 6 °C at 12:00 and 7 °C at 16:00. Daytime AT ranges from 25 °C to 33 °C, with a median value exceeding 30 °C.

MRT and PET at a height of 1.8 m at 16 pm and (b) hourly PET values in four receptor points.

During this period, thermal sensation throughout the area shifts from slight to extreme heat stress. Receptor points were positioned at the center of street segments (Fig. 9b). Among these, P2 shows a noticeably higher AT due to the lack of shading, with values comparable to those in the open squares.

MRT at 15:00 is generally similar across streets, with the exception of P1, which is approximately 5 °C lower than the others. MRT values in the squares are significantly higher than those observed in the streets, a trend mirrored in the PET values, which also show a pronounced increase in the squares relative to the surrounding street network.

3.3.4. Residential neighbourhood (A4)

The results show that the highest values of PET occur in the spaces in between the buildings where ventilation is blocked (Fig. 10a). While during the night and early morning, AT is quite homogeneous in the area, during the hottest hours several variations occur. The hotspots in this area are located in front of west facades and in weakly ventilated areas. The incoming shortwave radiation is not blocked by tree canopies, while larger shade is provided by the buildings.

The PET values of the four points under consideration are found to be relatively uniform during nocturnal hours (Fig. 10b); however, a divergence in values becomes apparent during daylight hours, with the maximum values recorded between 13:00 and 16:00 (54°C). P3, spanning the time period from 7:00 to 13:00, exhibits lower PET values in comparison to the other points. P2 reaches the maximum peak of PET values at 13:00, but it declines earlier than the other points.

3.4. Urban cooling from vegetation

During the day, reducing MRT with urban geometry seems more

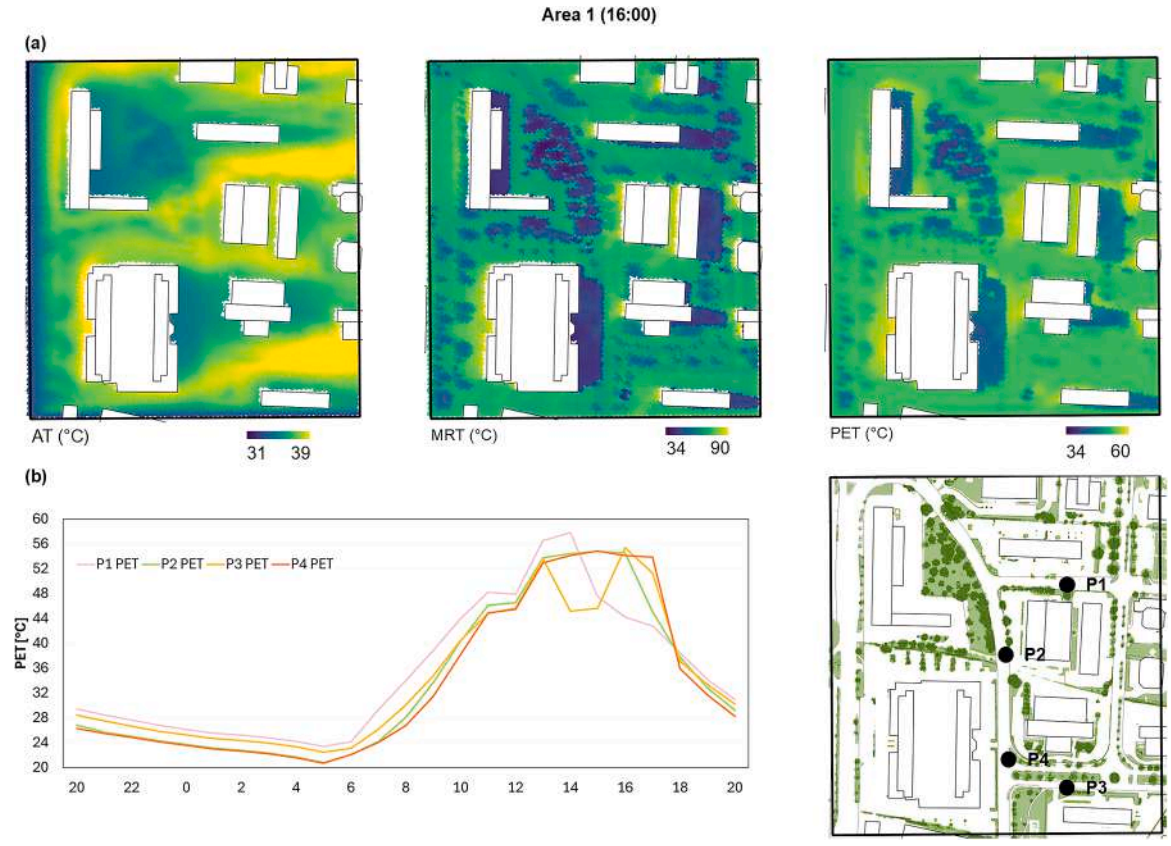

Fig. 7. Simulation results of A1: (a) Spatial distribution of AT, MRT and PET at a height of 1.8 m at 16 pm and (b) hourly PET values in four receptor points.

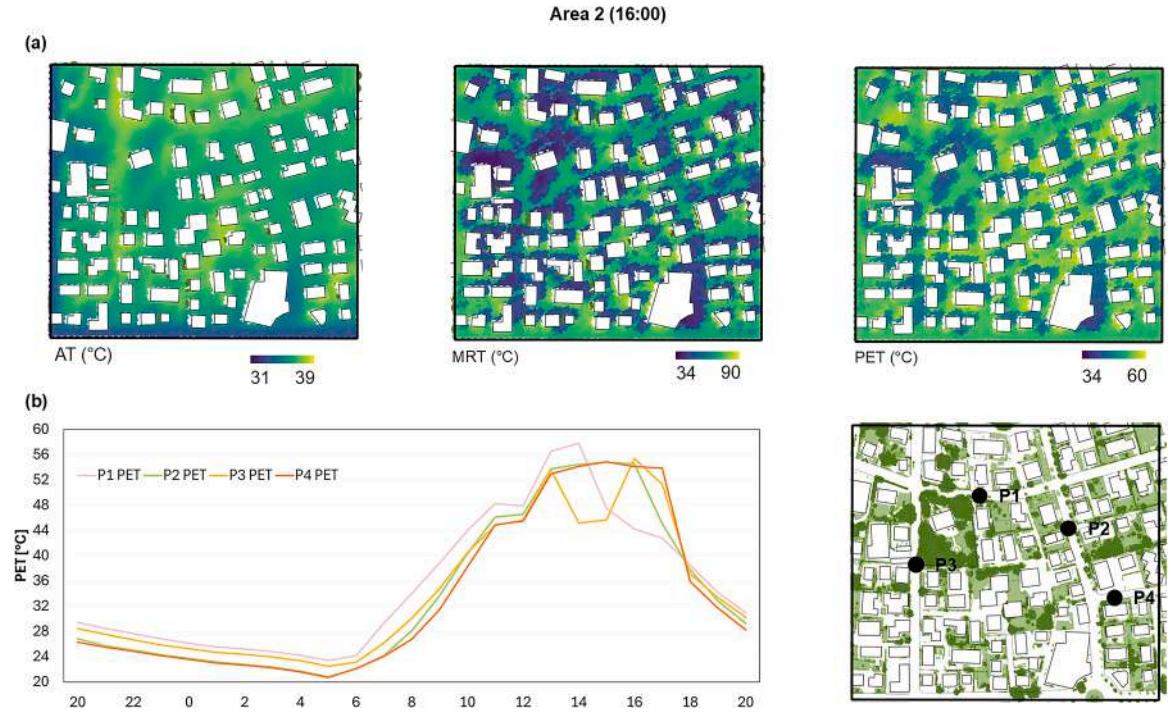

Fig. 8. Simulation results of A2: (a) Spatial distribution of AT, MRT and PET at a height of 1.8 m at 16 pm and (b) hourly PET values in four receptor points.

effective than tree planting. In A3, the high values of H/W ratio reduce the pedestrian thermal comfort more than with tree cover. However, AT, MRT and PET reduction by planting trees is effective in A1 and A2. The two areas have two different types of vegetation: in A1, the cooling is mainly given by a wide area with tall trees, while in A2 by a distributed system of private gardens with trees. Fig. 11 depicts the diurnal temperature reductions, calculated as no-green scenario results minus current scenario results, in the four areas due to urban greenery. The

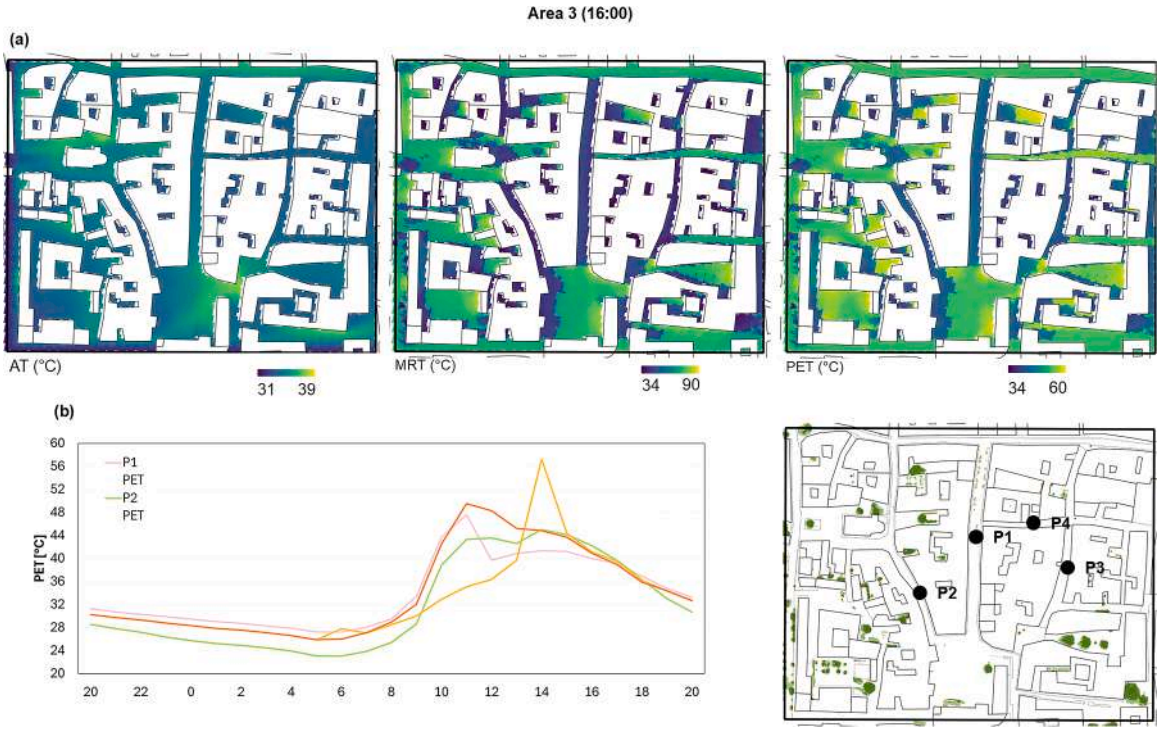

Fig. 9. Simulation results of A3: (a) Spatial distribution of AT, MRT and PET at a height of 1.8 m at 16 pm and (b) hourly PET values in four receptor points.

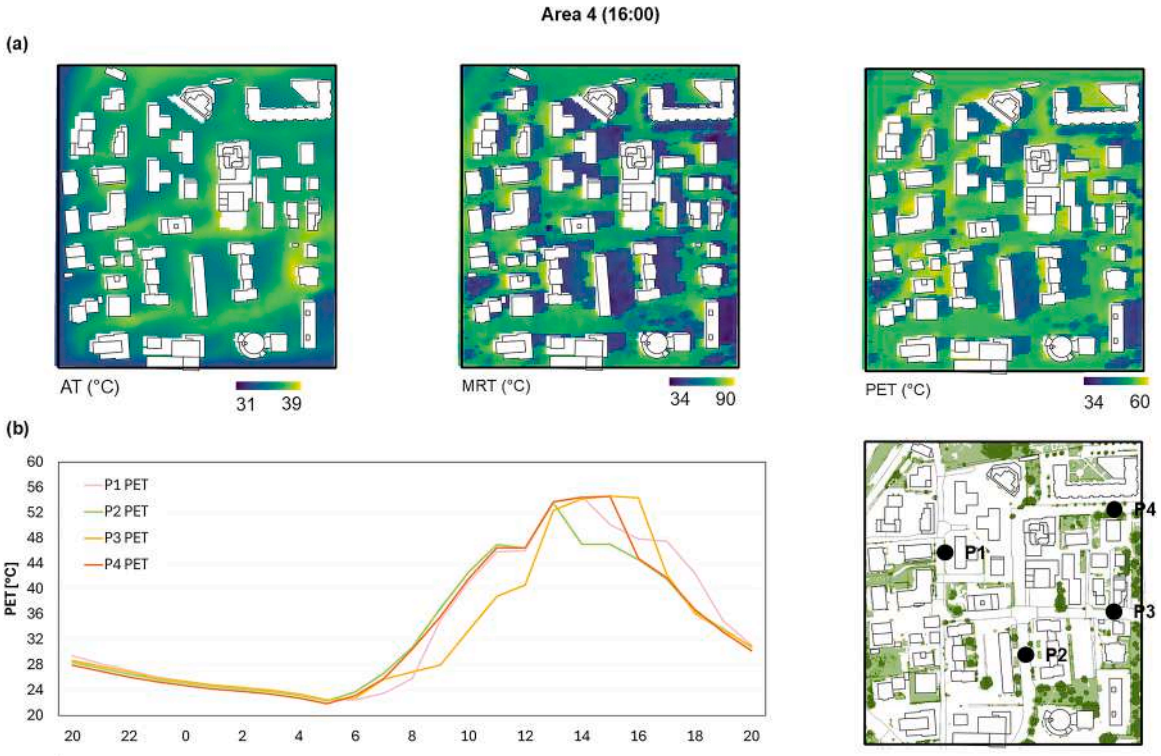

Fig. 10. Simulation results of A4: (a) Spatial distribution of AT, MRT and PET at a height of 1.8 m at 16 pm and (b) hourly PET values in four receptor points.

diurnal cooling efficiency of each scenario is homogeneous: it is increasingly effective during the morning reaching the maximum between 16:00-17:00, and then increasingly reducing during the night. In terms of MRT, the maximum variation is also achieved by A1 between 17:00 and 18:00, while in A2 and A4 the maximum variation is achieved between 16:00 and 17:00, in A4 it is achieved between 13:00 and 14:00. In terms of PET, the maximum variation is achieved by A1 between 18:00 and 19:00. While in A1 and A2, the variation is significant, in A3 and A4 is not significant.

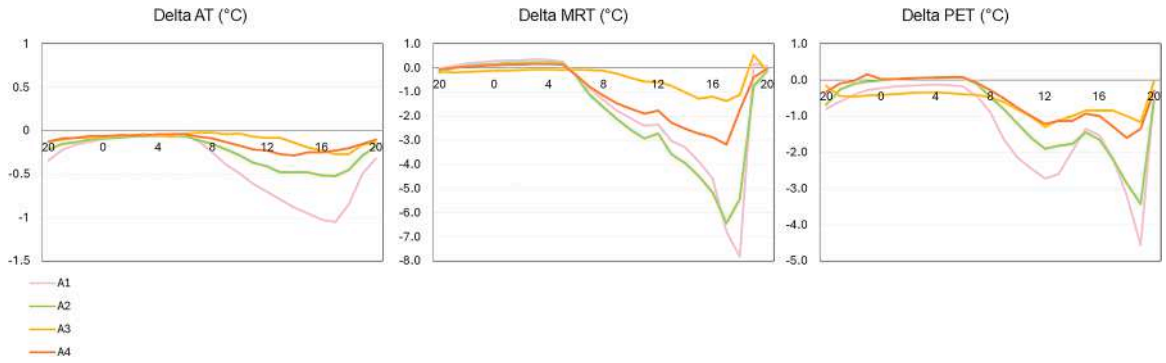

Fig. 11. Diurnal air temperature (on the left), mean radiant temperature (in the center) and physiological equivalent temperature (on the right) reductions (ΔAT, ΔMRT, and ΔPET) by each scenario. Reductions are calculated as the no-green scenario minus the green scenario. Negative values represent temperature reductions, which indicates the temperature reduction by the applied greenery.

3.5. Future weather scenarios

The differences between SQ and FW results are presented in Fig. 12. With the climate projection RCP8.5 of future scenarios, as expected, the increase is so high that PET in the areas is always higher than in the current scenario, with ranges between 2.71°C and 10.55°C in A1, 4.06°C and 9.67°C in A2, 4.06°C and 8.83°C in A3, and 3.31°C and 9.96°C in A4. Also the projected values of AT and MRT are always higher than the current scenarios, varying between 3.65°C and 6.75°C in AT and 3.33°C and 9.97°C in MRT. The highest difference is observed at 17:00 for AT, at 14:00 for MRT, and at 20:00 for PET.

To better understand these results, the differences between the current scenario and the future climate are investigated in all the study areas through maps and visualisation of the results at specific points. For brevity, only the results obtained for A1 are reported in Fig. A.3, with a summary of the results provided below. Within each area, some zones display greater differences. Despite green areas remaining places with lower PET values, they are also the areas most affected by the increase in PET. In relation to AT and RH, there are no major variations in each area, with homogeneous increases and decreases respectively between SQ and FW. In terms of MRT, the results show an increase in the absolute difference from SQ to FW, with surfaces exposed to the sun increasing more than shaded surfaces.

4. Discussion

This section discusses the results, paying particular attention to the variations between and within the four selected areas, and to the methodology for multi-area assessment. Specifically, it looks at variability between LCZs in Trento, the impact of vegetation and urban canyons on pedestrian thermal comfort, and the strengths and limitations of the proposed workflow.

4.1. Microclimate variations between LCZs in the Alpine context

This study allowed a comparison between microclimate parameters of different urban fabric in the city of Trento. The comparison of the meteorological and OTC conditions between the various LCZs of Trento

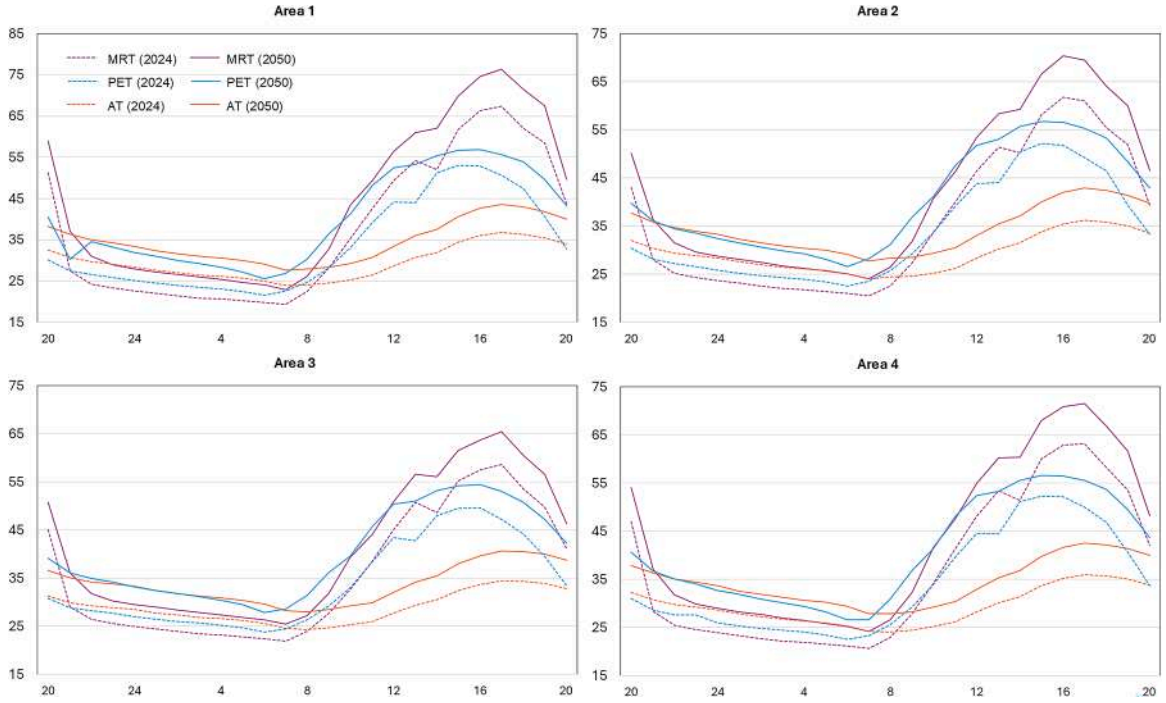

Fig. 12. Diurnal AT, MRT and PET variations between SQ and FS in each scenario. The 2050 scenarios are represented by solid lines, the 2024 scenarios are indicated by dashed lines.

revealed notable variations. However, it was found that intra-areas differences are more significant, especially between built-up areas and green or shaded areas.

Significant AT differences are observed during the hottest hours, with a maximum difference of 2.4°C between A3 (LCZ2) and A1 (LCZ8). The difference between mean AT in LCZ 8, LCZ 5 and LCZ 6 is low during daytime. These values are consistent with those reported in previous studies of European cities including differences of up to 1°C in Ghent (Top et al., 2020), Toulouse (Kwok et al., 2019), Barcelona (Hidalgo García & Arco Díaz, 2023), and Djoun (Richard et al., 2018). Nocturnal AT differences are smaller, as evidenced by the maximum difference of 0.55°C observed in our study. This finding aligns with observations presented in Milošević et al. (2021), which demonstrate that nocturnal temperature variations are significantly higher between vegetated and built-up LCZs, with LCZ9 exhibiting characteristics akin to the former category. The nocturnal thermal anomalies observed in this study are consistent with those reported in other European cities, such as Dublin (1-2°C for LCZ2; −1–0°C for LCZ 5 and LCZ 6). However, AT differences both during daytime and nighttime between built-LCZs in other studies and our investigation may vary according to the specific configuration of the LCZ. For instance, in Richard et al. (2018), LCZ 5 experienced a 1.3°C decrease during nighttime compared to LCZ6.

Furthermore, substantial disparities in terms of MRT are also observed during the hottest hours, ranging between 6°C and 8°C. These variations in MRT consequently result in significant differences in PET, underscoring the significance of radiation and wind speed (related to geometry) as pivotal factors for OTC. Indeed, during daytime the historical center appears to be the least uncomfortable area, confirming the key role of shading for OTC during daytime, as in the study of Kotharkar and Dongarsane (2024). The simulations indicate that citizens may experience extreme heat stress during daytime hours, with the highest mean PET reached in A1. In LCZ 8, LCZ 6, LC2, and LCZ 5, PET peaks reached 52,97°C, 51,79°C, 49,71°C and 52,16°C respectively. In contrast, LCZ 6 experiences a reduced duration of nighttime heat stress compared to the other LCZs. Consistent findings were reported in Antwerp, Brussels and Ghent (Verdonck et al., 2018).

Intra-areas differences are more significant, revealing the importance of geometry and of vegetation in reducing heat stress. During daytime, and particularly during the period of maximum heat accumulation, the maximum variability within areas occurs. Significant intra-variations are observed in several studies, such as Geletič et al. (2018) and Kwok et al. (2019). To further investigate this aspect, a future step of the research could correlate the thermal variables values to presence of vegetation (NDVI index) and surface temperature (LST) (Richard et al., 2018).

Finally, despite its alpine location, the temperature values obtained for Trento are comparable to those of other Italian cities in other contexts, e.g. in Catania by Detommaso et al. (2021), in Lecce by Gatto et al. (2021), in Perugia by Piselli et al. (2018), highlighting the importance of these studies in such areas.

4.2. Effect of urban canyons morphologies on thermal comfort

The comparison of microclimate results in different urban canyons helped to understand the effect of urban morphology on OTC as street canyons have a main role in controlling the amount of solar radiation received and reradiated by urban structures. Several studies mention H/W, street orientation, configuration and building typology, SVF, compactness, materials and surface coverage as key aspects for OTC. Shallow canyons receive more solar radiation leading to more thermal stress, confirming that when wide streets are planned, shading design strategies are necessary to reduce thermal stress, independently of the orientation (Ali-Toudert & Mayer, 2006). Narrow canyons present the most favourable comfort indices in summer (Chatzidimitriou & Yannas, 2017). Our study confirms that H/W ratio plays an important role in determining pedestrian-level thermal conditions. H/W ratio has a positive relationship with PET, but it should also keep in consideration the orientation (Jamei et al., 2016; Karimi et al., 2020). Indeed, the correlation between H/W and the mean of PET values during the hottest hours of the day shows that the urban canyon geometry and orientation are an important factor affecting microclimate. The results show that urban canyons with lower H/W ratio present the highest PET values due to increased solar radiation exposure. Similarly, the scattered diagram of the SVF against PET shows a strong correlation, indicating that daytime OTC is affected by geometry. Indeed, both parameters are closely linked to direct solar radiation, which has a strong correlation with daily PET values. Compared to solar radiation, the correlation between wind speed and PET values is weak (Fig. 13). In line with previous studies (Darbani et al., 2023; Nasrollahi et al., 2021; Srivanit & Jareemit, 2020), in dense scenarios (A3), east-west oriented canyons are exposed to higher heat stress levels in summer than north-south oriented canyons. The results show that compact urban geometry provides the best PET values during the day, but the worst during the night. The open-low rise instead gives the best results during the night, providing multiple hours without heat stress conditions. Indeed, during the day this district had limited shading provided by buildings. These results are in line with the findings of other studies (Kotharkar & Dongarsane, 2024).

Consistent shading with high H/W ratios is effective (Algeciras et al., 2016; Johansson & Emmanuel, 2006). This is in line with studies suggesting increasing shadow by increasing H/W ratios (Muniz-Gäal et al., 2020) in hot and arid climates (Darbani et al., 2023) but not only in hot and arid climates. E-W canyons need more protection from solar radiation, this protection could be with high H/W or also with trees with large crowns. Indeed, studies have investigated the positive effect of high LAI values, large trees and high truck trees in shallow canyons (Morakinyo et al., 2017).

4.3. Effect of vegetation on thermal comfort

The study allowed an understanding of the impact of urban greenery on OTC. Green elements are well known to have an important role in influencing microclimate parameters (Aram et al., 2019), especially providing better cooling effects on high-temperature asphalt surfaces (Pezzuto et al., 2022; Yan et al., 2023). The results show that in the hottest hours vegetation decreases AT and significantly decreases MRT and PET due to the shading of trees and their influence on radiative fluxes. These findings are aligned with Herath et al. (2024) emphasising the importance of spatial distribution and species selection and consistent with Darbani et al. (2023). Urban green, meant as grass and trees, reduces the interception of shortwave radiation by shading and covering the surface that would absorb heat.

Trees' cooling capacity depends on physical or structural characteristics, location and placement of trees (Morakinyo et al., 2017; Rahman et al., 2020). Canopy cover affects surface temperature reducing solar absorption (Imran et al., 2019; Rafiee et al., 2016). Several studies in urban areas proved the beneficial effects of trees and pervious surfaces observing reductions up to values between 5°C and 2.5°C (Battista et al., 2023; Chen et al., 2021; Cheng & Lin, 2024; Darvish et al., 2021). In this regard, areas protected by tree shadow have the more beneficial results, especially with large tree canopies (Guerri et al., 2023).

Our results show that in A1 RH and WS have significant increases from NV to SQ, while A2 has a significant variation of RH. In A1 the predominance of impervious surfaces and the scarcity of vegetation influence thermal stress conditions. However, the large green area protected by trees has a significant impact in improving thermal conditions. Indeed, A1 shows the greatest cooling effects due to vegetation, despite the low amount of green areas (around 6%). As size of small urban green areas, followed by shape and spatial distribution, is an important factor for cooling (Wu et al., 2025), the presence of a wide green area with many trees of a height above 12 m has a significant role in cooling the area. Thermal conditions in A2 are widely determined by the presence of vegetation, this is consistent with studies showing that trees are more

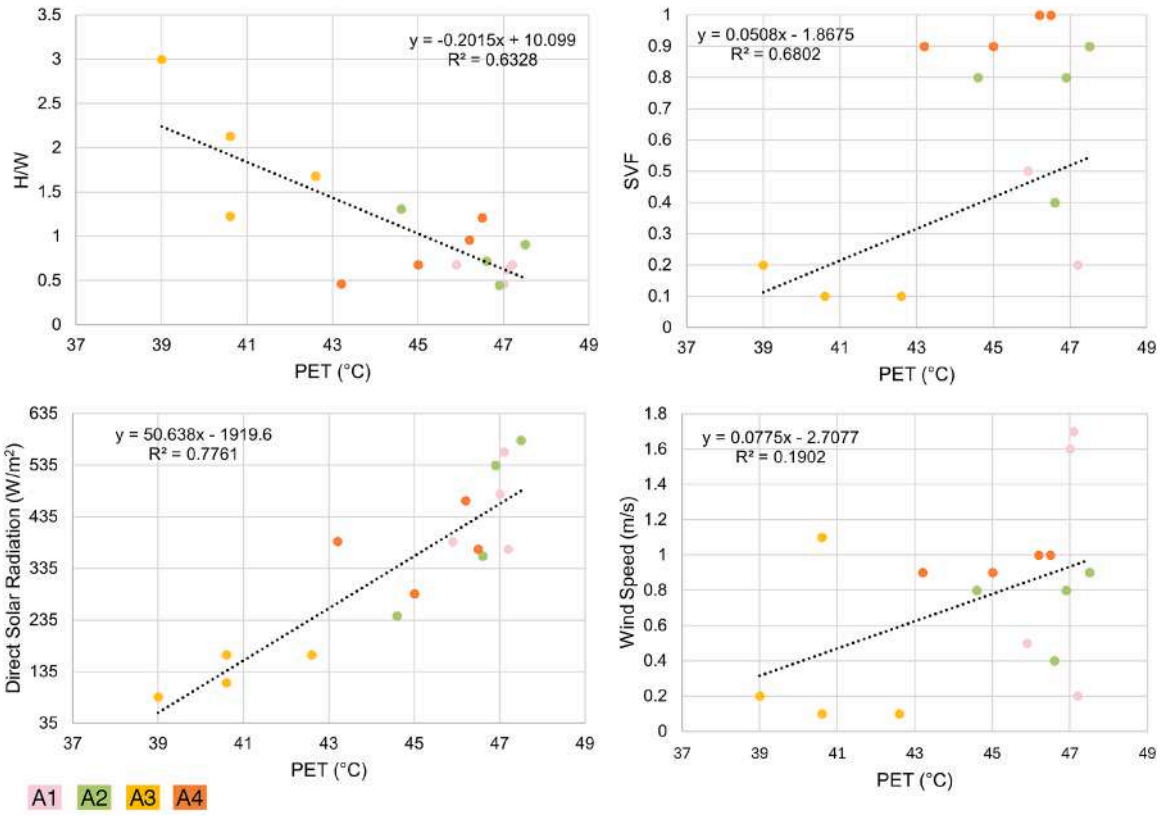

Fig. 13. Correlation trend between PET and H/W, direct solar radiation, and wind speed values between 10:00 and 18:00 in the receptor points.

effective in low urban density areas than in compact urban areas (Imran et al., 2019). The type of urban green in this area has a different configuration, as it covers almost 30% of the surface but is characterized by low trees (mainly third category). The cooling effect derived by vegetation in this area is significant, but lower compared to A1, suggesting that the dimension of the trees and the dimension of green areas are the most influential factors. Tree canopy cover is the dominant cooling factor according to(Zaerpour et al. (2025). The tree categorization that we have adopted is directly linked to tree canopy cover, as it accounts for tree height and foliage, but the analysis could be enhanced with more detailed canopy characteristics.

4.4. *Effect of climate change projections*

The simulation results of thermal comfort of the current configuration and weather conditions (SQ) and the future projections (FS) allowed an understanding of the impact of climate change. Climate change projections produce such an impact that the PET results in the area are always higher in FS than SQ. The results of the simulations, when compared with the study by Sola-Caraballo et al. (2024), show similar values: a significant temperature increase of up to 7°C is registered. The temperature increase is quite uniform within the area, but it shows that the presence of vegetation is not sufficient to improve OTC. In contrast, the study by Abedrabboh et al. (2025), based in Qatar, shows a lower increase in AT (1.98–2.58°C) and PET (0.34–2.65°C). However, the selected area in the latter study has a different climate and a denser urban configuration, with no vegetation. However, also this study demonstrated a declining effect in providing OTC by vegetation due to the increase in AT and decrease in RH. The analysis was conducted under the most pessimistic IPCC scenario (RPC 8.5), which is useful for assessing the worst-case outcomes in the absence of mitigation and adaptation strategies. Nevertheless, future work could benefit from also simulating less extreme scenarios to capture a broader range of possible future conditions and climate adaptation and mitigation perspectives.

The study applies the RCP8.5 scenario, the most unfavourable. Although it could be difficult to predict the exact situation in 2050, this scenario provides contrasted data on the worst expected situation. Future improvements from this perspective could improve the results of the study. For example, using local-specific future weather scenarios or adopting the recent SSP-based scenarios (e.g. SSP2–4.5, SSP5–8.5) could increase the precision of the results. The use of tools morphing existing EPW weather data with the HadCM3 climate change predictions underscores limitations and uncertainties. For example, the use of present day weather data can cause under- or over-estimations of climate change impacts or uncertainties related to microclimatic conditions. However, the tool offers a practical approach whose applicability is considered consistent (Belcher et al., 2005; Jentsch et al., 2013). Moreover, the temperature increase values refer to the simulated day representing an extremely hot summer day. Further analysis could expand the results over other seasons and weather times to represent less extreme conditions. Considering these aspects, the results are consistent with climate scenarios for the Autonomous Province of Trento provided by the climate model ensembles of Napoli et al. (2026). A direct comparison cannot be performed due to differences in the temporal frame and in the climate models. However, as qualitative considerations, the values of temperature increase in our results are within the ranges of the strongest increases among the ensemble. These high values support the evidence that the European Alps' air temperature has increased by more than 2°C compared to the pre-industrial period and is expected to undergo greater changes than the global average (Dumont et al., 2025).

4.5. *Strength and limitations of the multiscale workflow*

In this study, although each ENVI-met model was configured with its own specific boundary conditions, these were all derived from a single input dataset, which was processed and re-elaborated through the UWG tool. This approach ensured consistency in the baseline climatic input while allowing for localized differentiations based on the characteristics

of each area, particularly according to their respective LCZ and the UHI effect.

Moreover, as ENVI-met requires notable computation efforts, the simulation was performed for 24 hours representing one of the hottest days. Yet, this procedure does not capture the full variability of summer conditions. Including simulations of representative summer days would enhance the robustness of the results. These simplifications are due to the inability to perform dynamic simulations and the computational efforts derived by the use of ENVI-met. To improve the accuracy of model evaluation, a denser network of monitoring stations would be beneficial. Moreover, the assumption of constant wind speed may oversimplify conditions in a valley city, where local wind patterns such as thermal breezes can play a significant role.

Finally, future research should further disentangle the influence of vegetation and urban geometry on microclimatic outcomes, particularly across LCZs, while also considering the thermal properties of surface materials to better understand which factors most significantly drive urban temperature dynamics.

4.6. Limitations of the study

While the results of the status quo models were validated and suggest reasonable reliability, the observed discrepancies are either due to model limitations or the quality of input data. Regarding the latter, thermal properties of building walls, roofs and surfaces were assumed in our model, based on field visits and data derived by the Municipality. Given the amount of trees and the dimensions of the domains, trees were modelled starting from the built-in library considering geometrical characteristics. Other characteristics, such as LAI, foliage shortwave albedo and transmittance were not modified from the library. Including these data could give more accurate results, as LAD is a significant parameter (Liu et al., 2023). While using fixed wind conditions as ENVI-met inputs is a common practice especially for model domains (Dong et al., 2023; Patle & Ghuhe, 2025), the resulting air temperature might be affected by considering wind direction as forcing data constant (Eingrüber et al., 2023). Moreover, static cloud-free conditions may be responsible for overestimation of incoming solar radiation and solar-dependent parameters.

Validation through in-situ measurements is vital to ensure the robustness of results. While the most frequently validated meteorological variables are AT and RH (Liu et al., 2021), evaluating other variables such as MRT, SR, WS or PET could strengthen the results. In this study, the validation procedure was designed according to the availability of measurement tools (i.e. four sensors measuring simultaneously) and safety reasons, as the devices were unattended. Moreover, while several studies assessing multiple areas do not validate a receptor point in each area (e.g. Kotharkar & Dongarsane 2024; Salehi & Nasrollahi 2024; Herath et al., 2024), we provided a procedure ensuring validation in all analysis domains. As the workflow is intended as a single urban model, with a single climatic input and discretized in four areas, the simulation requires multiple simultaneous validation points (heterogeneity) reinforcing validity and robustness of the model compared to previous literature studies using single validation points. However, multiple validation points within each area could strengthen the findings.

5. Conclusions

This research aims to provide operative and methodological knowledge to climate sensitive urban planning with the assessment of summer pedestrian comfort. Driven by the need for context-based approaches, this study makes a valuable contribution to urban planning by providing a novel framework for multiple areas assessment through an effective workflow. The study examines the impact of urban geometry, vegetation, and future climate projections on microclimate conditions in Trento, an Alpine city whose context has not yet been explored in terms of summer pedestrian comfort. Instead of using field measurement data, we present a sound workflow morphing rural weather into context-specific data, simplifying the process of meteorological input for the model. We simulated microclimate parameters and outdoor thermal indexes in four neighbourhoods of Trento with current conditions, with scenarios without vegetation and with future climate projections to investigate the role of spatial configuration and offer key insights into the factors contributing to thermal discomfort.

The main outcomes are:

1) Variations in thermal stress exist between types of LCZs. Compact areas (historical center) showed higher levels of thermal stress during night-time, while slightly lower thermal stress during the day, highlighting the role of shade provided by urban fabric during daytime. Open areas showed lower thermal stress values during the night (RQ1).
2) The effect of vegetation is relevant in reducing night-time thermal stress in open areas. In terms of configuration, the case study with a large green area demonstrates the larger cooling effect provided by vegetation, followed by the neighbourhood with a distributed system of private gardens. Regarding geometry, areas with higher H/W ratios showed enhanced comfort during peak heat hours, while shaded orientations further improved thermal conditions. Notably, MRT was found to be a dominant factor in determining thermal comfort, underlining the importance of managing solar exposure and surface radiative properties in urban design. Future climate projections reveal that all areas will experience strong and extreme heat stress conditions during the daytime, highlighting the importance of selecting adaptation strategies (RQ2).
3) The proposed framework is effective as it provides validated spatial and climatic data obtained through simulations useful to develop local specific design recommendations. The workflow can be applied to other regions and can be the base to determine and test suitable adaptation strategies. This approach enables a sound understanding of how local context influences OTC, with a focus on the impact of vegetation and urban geometry, facilitating multiple areas assessments (RQ3).

The implications of these findings are relevant for climate sensitive urban planning and design. The results demonstrate that considerable differences exist between urban areas - even within the same city - due to variations in morphology, vegetation and microclimatic conditions. Our findings show that acknowledging these local variations can enable more targeted and effective strategies, such as defining intervention priorities and differentiating building requirements or adaptation measures tailored to each zone.

Key strategies emerging from the analysis include increasing vegetation and tree coverage, optimizing urban geometry with higher height-to-width (H/W) ratios, and improving shading through building orientation.

Despite quantity, the spatial arrangement of vegetation has an impact on thermal stress:

- Large green areas can significantly contribute to reduce night-time thermal stress in urban typologies with impervious surfaces;
- A system of well-distributed gardens with trees can reduce night-time thermal stress in areas with low-rise buildings.

The impacts of the greening types might differ also according to the type of urban typology, showing that there is not a universal solution that can fit all built-up types.

Urban geometry factors such as orientation and aspect ratio influence shading and ventilation significantly affecting thermal stress:

- Increasing canyon width (or reducing H/W) increases thermal stress and therefore additional mitigation strategies are required;

- In compact areas thermal stress is significantly affected by shading of buildings and orientation of streets.

The study offers a novel perspective by focusing on an Alpine city, an underrepresented context in the literature on outdoor thermal comfort, despite its vulnerability to heat stress and to the impacts of climate change. The findings underscore the need for more research in similar environments to enable cross-comparison and to develop context-specific strategies. Overall, this research supports the development of context-sensitive, evidence-based planning strategies to reduce heat stress—especially in smaller Alpine cities increasingly affected by climate change.

Declaration of generative AI and AI-assisted technologies in the writing process

During the preparation of this work the author(s) used Deepl Write in order to rephrase and improve the readability of some parts. After using this tool/service, the author(s) reviewed and edited the content as needed and take(s) full responsibility for the content of the published article.

CRediT authorship contribution statement

Anna Codemo: Writing – review & editing, Writing – original draft, Visualization, Validation, Software, Resources, Methodology, Investigation, Formal analysis, Data curation, Conceptualization. **Gianluca Maracchini:** Writing – review & editing, Writing – original draft, Validation, Supervision, Software, Methodology, Investigation, Formal analysis, Data curation, Conceptualization. **Sara Favargiotti:** Writing – review & editing, Supervision. **Rossano Albatici:** Writing – review & editing, Supervision.

Declaration of competing interest

The authors declare that they have no known competing financial interests or personal relationships that could have appeared to influence the work reported in this paper.

Acknowledgements

This study was realised within the project “Climate sensitive urban regeneration” with financial support from the Caritro Foundation (Italy) under the framework Caritro postdoc. The authors would like to thank the urban planners at the Municipality of Trento for providing support and information.

Appendix

Table A.1 and Fig. A.1-A.3

Table A.1
Pervious surfaces percentage and dimensions of the trees according to the municipal categorization by area.

Area	A1	A2	A3	A4
Percentage of pervious surfaces	6%	30%	1%	18%
Trees of 3rd category (0-12 m)	198	268	38	153
Trees of 2nd category (12-18 m)	94	27	10	21
Trees of 1st category (>18 m)	5	29	3	5

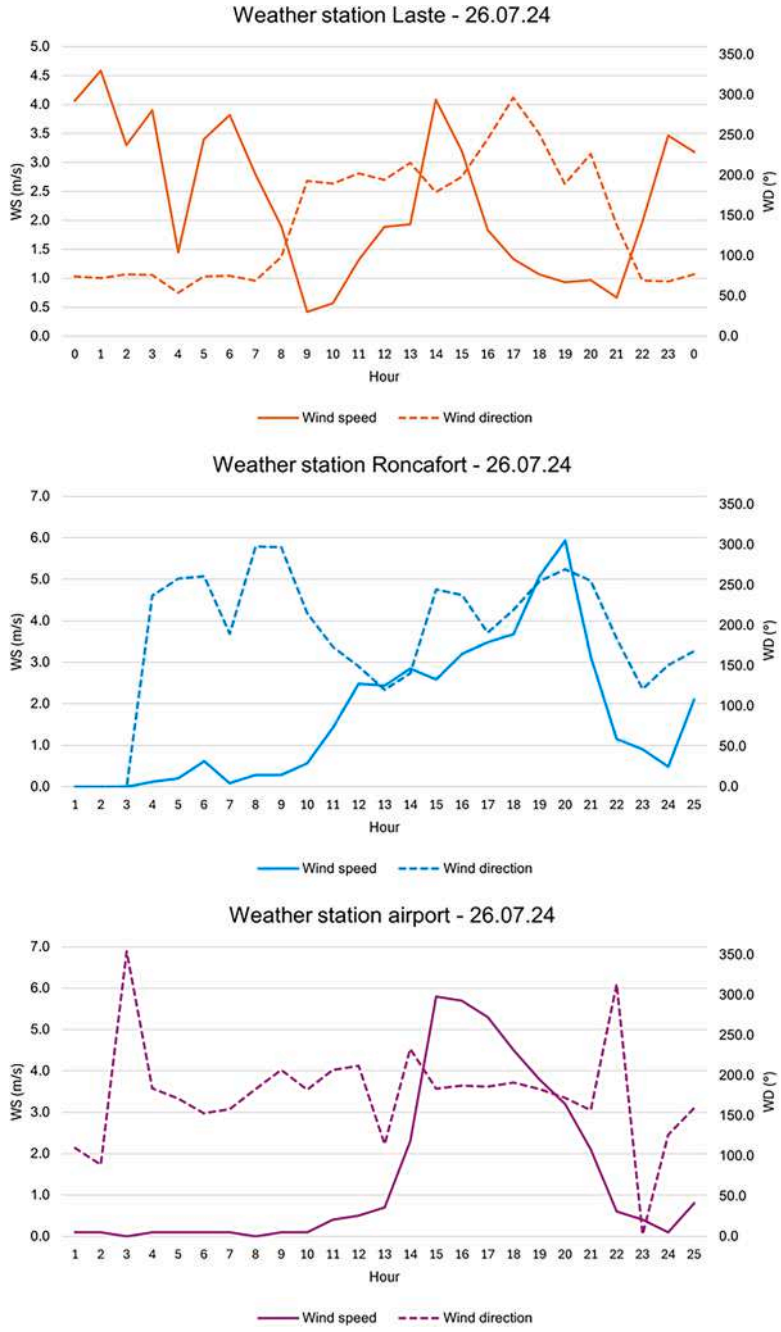

Fig. A.1. Wind speed and direction in the three weather stations on the selected day.

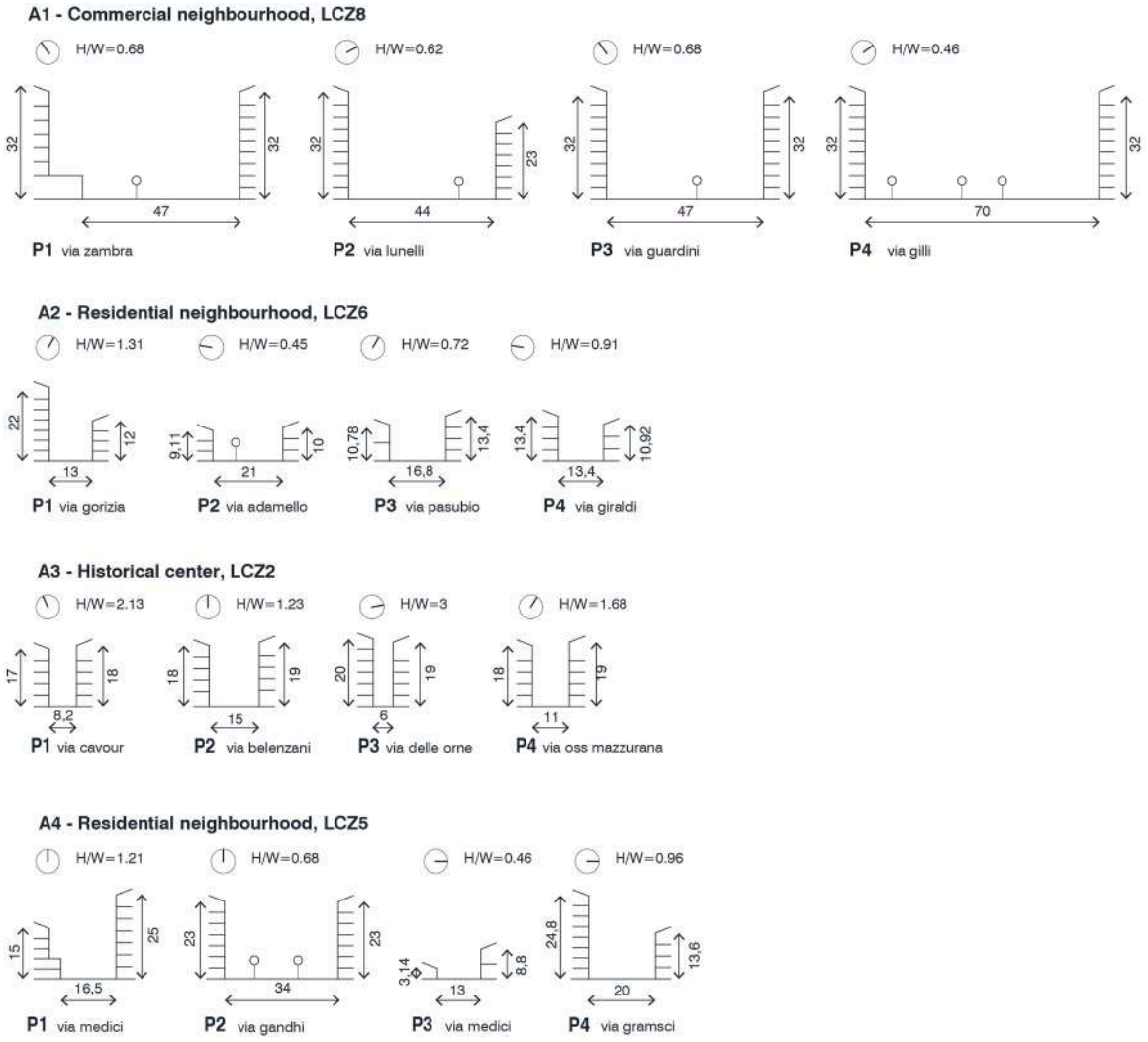

Fig. A.2. Orientation and H/W values of the receptor points in the four areas.

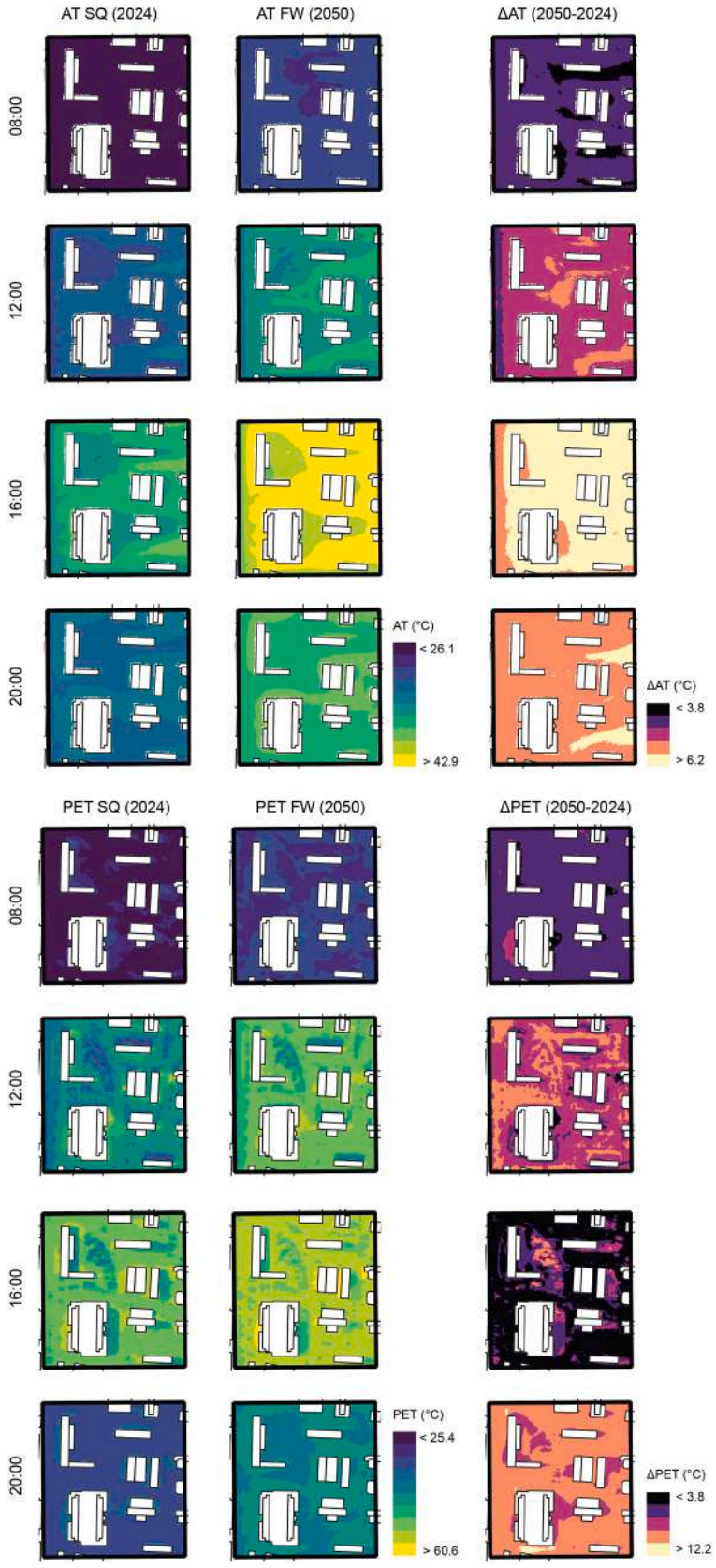

Fig. A.3. Simulated values of AT and PET in the SQ and FW scenarios, differences in terms of AT and PET between FW and SQ, calculated as values from 2050 minus values from 2024.

Data availability

Data will be made available on request.

References

Abedrabboh, O., Fountoukis, C., Al-Ansari, T., & Alfarra, M. R. (2025). Simulating microclimate adaptation: Evaluating heat mitigation strategies for Doha, Qatar, under current and future climate conditions. *Sustainable Cities and Society, 132*, Article 106777. https://doi.org/10.1016/j.scs.2025.106777

Alchapar, N. L., & Correa, E. N. (2016). The use of reflective materials as a strategy for urban cooling in an arid "OASIS" city. *Sustainable Cities and Society, 27*, 1–14.

Algeciras, J. A. R., Consuegra, L. G., & Matzarakis, A. (2016). Spatial-temporal study on the effects of urban street configurations on human thermal comfort in the world heritage city of Camagüey-Cuba. *Building and Environment, 101*, 85–101.

Ali-Toudert, F., & Mayer, H. (2006). Numerical study on the effects of aspect ratio and orientation of an urban street canyon on outdoor thermal comfort in hot and dry climate. *Building and Environment, 41*, 94–108.

Alsaad, H., Hartmann, M., Hilbel, R., & Voelker, C. (2022). ENVI-met validation data accompanied with simulation data of the impact of facade greening on the urban microclimate. *Data in Brief, 42*, Article 108200.

Aram, F., Higueras García, E., Solgi, E., & Mansournia, S. (2019). Urban green space cooling effect in cities. *Heliyon, 5*, Article e01339. https://doi.org/10.1016/j.heliyon.2019.e01339

Arrar, H. F., Kaoula, D., Santamouris, M., Foufa-Abdessemed, A., Emmanuel, R., Matallah, M. E., … Attia, S. (2024). Coupling of different nature base solutions for pedestrian thermal comfort in a Mediterranean climate. *Building and Environment, 256*, 111480.

Ascione, F., Böttcher, O., Manniti, G., Mastellone, M., & Mühle, J. (2024). The effect of climate change and urbanization on outdoor microclimate: A case study in Berlin. *Energy and Buildings, 308*, Article 114024.

ASHRAE, 2010. Thermal environmental conditions for human occupancy.

Banerjee, S., Pek, R. X. Y., Yik, S. K., Ching, G. N., Ho, X. T., Dzyuban, Y., Crank, P. J., Acero, J. A., & Chow, W. T. L. (2024). Assessing impact of urban densification on outdoor microclimate and thermal comfort using ENVI-met simulations for Combined Spatial-Climatic Design (CSCD) approach. *Sustainable Cities and Society, 105*, Article 105302. https://doi.org/10.1016/j.scs.2024.105302

Battista, G., Vollaro, E., de, L., Ocłoń, P., Vollaro, R., & de, L. (2023). Effects of urban heat island mitigation strategies in an urban square: A numerical modelling and experimental investigation. *Energy and Buildings, 282*, Article 112809. https://doi.org/10.1016/j.enbuild.2023.112809

Bechtel, B., Alexander, P. J., Beck, C., Böhner, J., Brousse, O., Ching, J., Demuzere, M., Fonte, C., Gál, T., & Hidalgo, J. (2019). Generating WUDAPT Level 0 data–current status of production and evaluation. *Urban Climate, 27*, 24–45.

Belcher, S., Hacker, J., & Powell, D. (2005). Constructing design weather data for future climates. *Building Services Engineering Research & Technology : BSER & T, 26*, 49–61. https://doi.org/10.1191/0143624405bt112oa

Bowler, D. E., Buyung-Ali, L., Knight, T. M., & Pullin, A. S. (2010). Urban greening to cool towns and cities: A systematic review of the empirical evidence. *Landscape and Urban Planning, 97*, 147–155. https://doi.org/10.1016/j.landurbplan.2010.05.006

Carnieletto, L., Ferrando, M., Teso, L., Sun, K., Zhang, W., Causone, F., Romagnoni, P., Zarrella, A., & Hong, T. (2021). Italian prototype building models for urban scale building performance simulation. *Building and Environment, 192*, Article 107590.

Chatzidimitriou, A., & Yannas, S. (2017). Street canyon design and improvement potential for urban open spaces; the influence of canyon aspect ratio and orientation on microclimate and outdoor comfort. *Sustainable Cities and Society, 33*, 85–101.

Chatzipoulka, C., Steemers, K., & Nikolopoulou, M. (2020). Density and coverage values as indicators of thermal diversity in open spaces: Comparative analysis of London and Paris based on sun and wind shadow maps. *Cities (London, England), 100*, Article 102645. https://doi.org/10.1016/j.cities.2020.102645

Chen, L., Kántor, N., & Nikolopoulou, M. (2022). Meta-analysis of outdoor thermal comfort surveys in different European cities using the RUROS database: The role of background climate and gender. *Energy and Buildings, 256*, Article 111757. https://doi.org/10.1016/j.enbuild.2021.111757

Chen, T., Yang, H., Chen, G., Lam, C. K. C., Hang, J., Wang, X., Liu, Y., & Ling, H. (2021). Integrated impacts of tree planting and aspect ratios on thermal environment in street canyons by scaled outdoor experiments. *Science of The Total Environment, 764*, Article 142920. https://doi.org/10.1016/j.scitotenv.2020.142920

Cheng, C. Y., & Lin, T. P. (2024). Decision tree analysis of thermal comfort in the courtyard of a senior residence in hot and humid climate. *Sustainable Cities and Society, 101*, Article 105165. https://doi.org/10.1016/j.scs.2023.105165

Cui, P., Jiang, J., Zhang, J., & Wang, L. (2023). Effect of street design on UHI and energy consumption based on vegetation and street aspect ratio: Taking Harbin as an example. *Sustainable Cities and Society, 92*, 104484. https://doi.org/10.1016/j.scs.2023.104484

Darbani, E. S., Rafieian, M., Parapari, D. M., & Guldmann, J.-M. (2023). Urban design strategies for summer and winter outdoor thermal comfort in arid regions: The case of historical, contemporary and modern urban areas in Mashhad, Iran. *Sustainable Cities and Society, 89*, Article 104339. https://doi.org/10.1016/j.scs.2022.104339

Darvish, A., Eghbali, G., & Eghbali, S. R. (2021). Tree-configuration and species effects on the indoor and outdoor thermal condition and energy performance of courtyard buildings. *Urban Climate, 37*, Article 100861. https://doi.org/10.1016/j.uclim.2021.100861

Detommaso, M., Costanzo, V., & Nocera, F. (2021). Application of weather data morphing for calibration of urban ENVI-met microclimate models. Results and critical issues. *Urban Climate, 38*, Article 100895. https://doi.org/10.1016/j.uclim.2021.100895

Dong, Q., Xu, X., & Zhen, M. (2023). Assessing the cooling and buildings' energy-saving potential of urban trees in severe cold region of China during summer. *Building and Environment, 244*, Article 110818. https://doi.org/10.1016/j.buildenv.2023.110818

Dumont, M., Monteiro, D., Filhol, S., Gascoin, S., Marty, C., Hagenmuller, P., Morin, S., Choler, P., & Thuiller, W. (2025). The European Alps in a changing climate: physical trends and impacts. *Comptes Rendus Géoscience, 357*, 25–42. https://doi.org/10.5802/crgeos.288

Ebrahimabadi, S., Nilsson, K. L., & Johansson, C. (2015). The Problems of Addressing Microclimate Factors in Urban Planning of the Subarctic Regions. *Environment and Planning B: Urban Analytics and City Science, 42*, 415–430. https://doi.org/10.1068/b130117p

Eingrüber, N., Korres, W., Löhnert, U., & Schneider, K. (2023). Investigation of the ENVI-met model sensitivity to different wind direction forcing data in a heterogeneous urban environment. *Advances in Science and Research, 20*, 65–71. https://doi.org/10.5194/asr-20-65-2023

Emery, J., Pohl, B., Crétat, J., Richard, Y., Pergaud, J., Rega, M., Zito, S., Dudek, J., Vairet, T., Joly, D., & Thévenin, T. (2021). How local climate zones influence urban air temperature: Measurements by bicycle in Dijon, France. *Urban Climate, 40*, Article 101017. https://doi.org/10.1016/j.uclim.2021.101017

Erell, E., Pearlmutter, D., Boneh, D., & Kutiel, P. B. (2014). Effect of high-albedo materials on pedestrian heat stress in urban street canyons. *Urban Climate, 10*, 367–386.

Fabbri, K., Antonini, E., & Marchi, L. (2023). Sun-shading sails in courtyards: An Italian case study with RayMan. *Sustainability, 15*, Article 13033. https://doi.org/10.3390/su151713033

Fiorillo, E., Brilli, L., Carotenuto, F., Cremonini, L., Gioli, B., Giordano, T., & Nardino, M. (2023). Diurnal outdoor thermal comfort mapping through envi-met simulations, remotely sensed and in situ measurements. *Atmosphere, 14*, 641. https://doi.org/10.3390/atmos14040641

Fu, H., Jiao, Y., Deng, L., & Wang, W. (2025). Dynamic impacts of vegetation growth and urban development on microclimate and building energy consumption. *Sustainable Cities and Society, 126*, Article 106382. https://doi.org/10.1016/j.scs.2025.106382

Gatto, E., Ippolito, F., Rispoli, G., Carlo, O. S., Santiago, J. L., Aarrevaara, E., Emmanuel, R., & Buccolieri, R. (2021). Analysis of urban greening scenarios for improving outdoor thermal comfort in neighbourhoods of Lecce (Southern Italy). *Climate, 9*, 116. https://doi.org/10.3390/cli9070116

Geletič, J., Lehnert, M., Savić, S., & Milošević, D. (2018). Modelled spatiotemporal variability of outdoor thermal comfort in local climate zones of the city of Brno, Czech Republic. *Science of The Total Environment, 624*, 385–395. https://doi.org/10.1016/j.scitotenv.2017.12.076

Georgakis, C., & Santamouris, M. (2006). Experimental investigation of air flow and temperature distribution in deep urban canyons for natural ventilation purposes. *Energy and Buildings, 38*, 367–376.

Gherri, B., Maiullari, D., Finizza, C., Maretto, M., & Naboni, E. (2021). On the Thermal Resilience of Venetian Open Spaces. *Heritage, 4*, 4286–4303. https://doi.org/10.3390/heritage4040236

Giovannini, L., Zardi, D., & De Franceschi, M. (2011). Analysis of the urban thermal fingerprint of the city of Trento in the Alps. *Journal of Applied Meteorology and Climatology, 50*, 1145–1162.

Grêt-Regamey, A., Altwegg, J., Sirén, E. A., van Strien, M. J., & Weibel, B. (2017). Integrating ecosystem services into spatial planning—a spatial decision support tool. *Landscape and Urban Planning, 165*, 206–219. https://doi.org/10.1016/j.landurbplan.2016.05.003

Guerri, G., Crisci, A., & Morabito, M. (2023). Urban microclimate simulations based on GIS data to mitigate thermal hot-spots: Tree design scenarios in an industrial area of Florence. *Building and Environment, 245*, Article 110854. https://doi.org/10.1016/j.buildenv.2023.110854

Halkos, G. E., & Gkampoura, E.-C. (2021). Evaluating the effect of economic crisis on energy poverty in Europe. *Renewable & Sustainable Energy Reviews, 144*, Article 110981. https://doi.org/10.1016/j.rser.2021.110981

Herath, P., Bai, X., Jin, H., & Thatcher, M. (2024). Does the spatial configuration of urban parks matter in ameliorating extreme heat? *Urban Climate, 53*, Article 101756. https://doi.org/10.1016/j.uclim.2023.101756

Heris, M. P., Middel, A., & Muller, B. (2020). Impacts of form and design policies on urban microclimate: Assessment of zoning and design guideline choices in urban redevelopment projects. *Landscape and Urban Planning, 202*, Article 103870. https://doi.org/10.1016/j.landurbplan.2020.103870

Hidalgo García, D., & Arco Díaz, J. (2023). Mitigation and resilience of local climatic zones to the effects of extreme heat: Study on the city of Barcelona (Spain). *Urban Science, 7*, 102.

Hurlimann, A., Moosavi, S., & Browne, G. R. (2021). Urban planning policy must do more to integrate climate change adaptation and mitigation actions. *Land Use Policy, 101*, Article 105188. https://doi.org/10.1016/j.landusepol.2020.105188

Imran, H. M., Kala, J., Ng, A. W. M., & Muthukumaran, S. (2019). Effectiveness of vegetated patches as green infrastructure in mitigating urban heat island effects during a heatwave event in the city of Melbourne. *Weather and Climate Extremes, 25*, Article 100217. https://doi.org/10.1016/j.wace.2019.100217

Core Writing Team IPCC. (2023). climate change 2023 synthesis report summary for policymakers, climate change 2023: synthesis report. In H. Lee, & J. Romero (Eds.), *Contribution of Working Groups I, II and III to the Sixth Assessment Report of the Intergovernmental Panel on Climate Change*. IPCC. Core Writing Team.

ISO, 2005. Ergonomics of the thermal environment: analytical determination and interpretation of thermal comfort using calculation of the PMV and PPD indices and local thermal comfort criteria.
Jamei, E., Rajagopalan, P., Seyedmahmoudian, M., & Jamei, Y. (2016). Review on the impact of urban geometry and pedestrian level greenING ON Outdoor thermal comfort. *Renewable & Sustainable Energy Reviews, 54*, 1002–1017. https://doi.org/10.1016/j.rser.2015.10.104
Jentsch, M.F., James, P., Bahaj, A., 2012. CCWorldWeatherGen software: Manual for CCWorldWeatherGen climate change world weather file generator.
Jentsch, M. F., James, P. A. B., Bourikas, L., & Bahaj, A. S. (2013). Transforming existing weather data for worldwide locations to enable energy and building performance simulation under future climates. *Renewable Energy, 55*, 514–524. https://doi.org/10.1016/j.renene.2012.12.049
Johansson, E., & Emmanuel, R. (2006). The influence of urban design on outdoor thermal comfort in the hot, humid city of Colombo, Sri Lanka. *International Journal of Biometeorology, 51*, 119–133.
Karimi, A., Sanaieian, H., Farhadi, H., & Norouzian-Maleki, S. (2020). Evaluation of the thermal indices and thermal comfort improvement by different vegetation species and materials in a medium-sized urban park. *Energy Reports, 6*, 1670–1684.
Kim, J., Yeom, S., & Hong, T. (2025). Analyzing the cooling effect, thermal comfort, and energy consumption of integrated arrangement of high-rise buildings and green spaces on urban heat island. *Sustainable Cities and Society, 119*, Article 106105. https://doi.org/10.1016/j.scs.2024.106105
Kleerekoper, L., Esch, M.van, & Salcedo, T. B. (2012). How to make a city climate-proof, addressing the urban heat island effect. *Resources, Conservation, and Recycling, 64*, 30–38. https://doi.org/10.1016/j.resconrec.2011.06.004
Kotharkar, R., & Dongarsane, P. (2024). Investigating outdoor thermal comfort variations across local climate zones in Nagpur, India, using ENVI-met. *Building and Environment, 249*, Article 111122. https://doi.org/10.1016/j.buildenv.2023.111122
Kotlarski, S., Gobiet, A., Morin, S., Olefs, M., Rajczak, J., & Samacoïts, R. (2023). 21st century alpine climate change. *Climate Dynamics, 60*, 65–86. https://doi.org/10.1007/s00382-022-06303-3
Kwok, Y. T., Schoetter, R., Lau, K. K., Hidalgo, J., Ren, C., Pigeon, G., & Masson, V. (2019). How well does the local climate zone scheme discern the thermal environment of Toulouse (France)? An analysis using numerical simulation data. *International Journal of Climatology : A Journal of the Royal Meteorological Society, 39*, 5292–5315.
Lafortezza, R., Chen, J., Van Den Bosch, C. K., & Randrup, T. B. (2018). Nature-based solutions for resilient landscapes and cities. *Environmental Research, 165*, 431–441. https://doi.org/10.1016/j.envres.2017.11.038
Lai, D., Liu, W., Gan, T., Liu, K., & Chen, Q. (2019). A review of mitigating strategies to improve the thermal environment and thermal comfort in urban outdoor spaces. *Science of The Total Environment, 661*, 337–353. https://doi.org/10.1016/j.scitotenv.2019.01.062
Lai, D., Liu, Y., Liao, M., & Yu, B. (2023). Effects of different tree layouts on outdoor thermal comfort of green space in summer Shanghai. *Urban Climate, 47*, Article 101398. https://doi.org/10.1016/j.uclim.2022.101398
Lam, C. K. C., Lee, H., Yang, S.-R., & Park, S. (2021). A review on the significance and perspective of the numerical simulations of outdoor thermal environment. *Sustainable Cities and Society, 71*, Article 102971. https://doi.org/10.1016/j.scs.2021.102971
Lam, C. K. C., Shooshtarian, S., & Kenawy, I. (2023). Assessment of urban physical features on summer thermal perceptions using the local climate zone classification. *Building and Environment, 236*, Article 110265. https://doi.org/10.1016/j.buildenv.2023.110265
Lau, K. K.-L., Chung, S. C., & Ren, C. (2019). Outdoor thermal comfort in different urban settings of sub-tropical high-density cities: An approach of adopting local climate zone (LCZ) classification. *Building and Environment, 154*, 227–238. https://doi.org/10.1016/j.buildenv.2019.03.005
Leconte, F., Bouyer, J., Claverie, R., & Pétrissans, M. (2015). Using Local Climate Zone scheme for UHI assessment: Evaluation of the method using mobile measurements. *Building and Environment, 83*, 39–49. https://doi.org/10.1016/j.buildenv.2014.05.005
Lee, W., Bell, M. L., Gasparrini, A., Armstrong, B. G., Sera, F., Hwang, S., Lavigne, E., Zanobetti, A., Coelho, M., de, S. Z. S., Saldiva, P. H. N., Osorio, S., Tobias, A., Zeka, A., Goodman, P. G., Forsberg, B., Rocklöv, J., Hashizume, M., Honda, Y., Guo, Y.-L. L., Seposo, X., Dung, D. V., Dang, T. N., Tong, S., Guo, Y., & Kim, H. (2018). Mortality burden of diurnal temperature range and its temporal changes: A multi-country study. *Environment International, 110*, 123–130. https://doi.org/10.1016/j.envint.2017.10.018
Li, Y., Lin, D., Zhang, Y., Song, Z., Sha, X., Zhou, S., Chen, C., & Yu, Z. (2023). Quantifying tree canopy coverage threshold of typical residential quarters considering human thermal comfort and heat dynamics under extreme heat. *Building and Environment, 233*, Article 110100. https://doi.org/10.1016/j.buildenv.2023.110100
Liu, L., Lin, Y., Xiao, Y., Xue, P., Shi, L., Chen, X., & Liu, J. (2018). Quantitative effects of urban spatial characteristics on outdoor thermal comfort based on the LCZ scheme. *Building and Environment, 143*, 443–460. https://doi.org/10.1016/j.buildenv.2018.07.019
LIU, L., & WU, J. (2022). Scenario analysis in urban ecosystem services research: Progress, prospects, and implications for urban planning and management. *Landscape and Urban Planning, 224*, Article 104433. https://doi.org/10.1016/j.landurbplan.2022.104433
Liu, Z., Cheng, K. Y., Sinsel, T., Simon, H., Jim, C. Y., Morakinyo, T. E., He, Y., Yin, S., Ouyang, W., Shi, Y., & Ng, E. (2023). Modeling microclimatic effects of trees and green roofs/façades in ENVI-met: Sensitivity tests and proposed model library. *Building and Environment, 244*, Article 110759. https://doi.org/10.1016/j.buildenv.2023.110759
Liu, Z., Cheng, W., Jim, C. Y., Morakinyo, T. E., Shi, Y., & Ng, E. (2021). Heat mitigation benefits of urban green and blue infrastructures: A systematic review of modeling techniques, validation and scenario simulation in ENVI-met V4. *Building and Environment, 200*, Article 107939. https://doi.org/10.1016/j.buildenv.2021.107939
Lobaccaro, G., & Acero, J. A. (2015). Comparative analysis of green actions to improve outdoor thermal comfort inside typical urban street canyons. *Urban Climate, 14*, 251–267.
López-Cabeza, V. P., Rivera-Gómez, C., Roa-Fernández, J., Hernandez-Valencia, M., & Herrera-Limones, R. (2023). Effect of thermal inertia and natural ventilation on user comfort in courtyards under warm summer conditions. *Building and Environment, 228*, Article 109812. https://doi.org/10.1016/j.buildenv.2022.109812
Luo, Y., Wu, Z., Wong, M. S., Yang, J., & Jiao, Z. (2024). Simulating the impact of ventilation corridors for cooling air temperature in local climate zone scheme. *Sustainable Cities and Society, 115*, Article 105848. https://doi.org/10.1016/j.scs.2024.105848
Ma, F., Jin, Y., Baek, S., & Yoon, H. (2023). Influence of path design cooling strategies on thermal conditions and pedestrian walkability in high-rise residential complexes. *Urban Forestry & Urban Greening, 86*, Article 127981. https://doi.org/10.1016/j.ufug.2023.127981
Mackey, C., Vasanthakumar, S., Dao, A., 2020. The Urban Weather Generator (UWG).
Magli, S., Lodi, C., Lombroso, L., Muscio, A., & Teggi, S. (2015). Analysis of the urban heat island effects on building energy consumption. *International Journal of Energy and Environmental Engineering, 6*, 91–99.
Mao, J., Yang, J. H., Afshari, A., & Norford, L. K. (2017). Global sensitivity analysis of an urban microclimate system under uncertainty: Design and case study. *Building and Environment, 124*, 153–170. https://doi.org/10.1016/j.buildenv.2017.08.011
Maracchini, G., Bavarsad, F. S., Di Giuseppe, E., & D'Orazio, M. (2022). Sensitivity and uncertainty analysis on urban heat island intensity using the local climate zone (LCZ) schema: The case study of Athens. In *Presented at the International Conference on Sustainability in Energy and Buildings* (pp. 281–290). Springer.
Marchi, L., Gaspari, J., & Fabbri, K. (2023). Outdoor microclimate in courtyard buildings: impact of building perimeter configuration and tree density. *Buildings, 13*, 2687. https://doi.org/10.3390/buildings13112687
Matzarakis, A., Mayer, H., & Iziomon, M. G. (1999). Applications of a universal thermal index: physiological equivalent temperature. *International Journal of Biometeorology, 43*, 76–84.
Middel, A., Häb, K., Brazel, A. J., Martin, C. A., & Guhathakurta, S. (2014). Impact of urban form and design on mid-afternoon microclimate in Phoenix Local Climate Zones. *Landscape and Urban Planning, 122*, 16–28.
Milošević, D., Savić, S., Kresoja, M., Lužanin, Z., Šećerov, I., Arsenović, D., Dunjić, J., & Matzarakis, A. (2021). Analysis of air temperature dynamics in the "local climate zones" of Novi Sad (Serbia) based on long-term database from an urban meteorological network. *International Journal of Biometeorology*, 1–14.
Morakinyo, T. E., Kong, L., Lau, K. K. L., Yuan, C., & Ng, E. (2017). A study on the impact of shadow-cast and tree species on in-canyon and neighborhood's thermal comfort. *Building and Environment, 115*, 1–17.
Morakinyo, T. E., & Lam, Y. F. (2016). Simulation study on the impact of tree-configuration, planting pattern and wind condition on street-canyon's micro-climate and thermal comfort. *Building and Environment, 103*, 262–275.
Moriasi, N. D., Arnold, J. G., Van Liew, M. W., Bingner, R. L., Harmel, R. D., & Veith, T. L. (2007). Model evaluation guidelines for systematic quantification of accuracy in watershed simulations. *Transactions of the ASABE, 50*, 885–900. https://doi.org/10.13031/2013.23153
Morlot, M., Russo, S., Feyen, L., & Formetta, G. (2023). Trends in heat and cold wave risks for the Italian Trentino-Alto Adige region from 1980 to 2018. *Natural Hazards and Earth System Sciences, 23*, 2593–2606.
Motie, M. B., Yeganeh, M., & Bemanian, M. (2023). Assessment of greenery in urban canyons to enhance thermal comfort & air quality in an integrated seasonal model. *Applied Geography (Sevenoaks, England), 151*, Article 102861.
Muniz-Gäal, L. P., Pezzuto, C. C., de Carvalho, M. F. H., & Mota, L. T. M. (2020). Urban geometry and the microclimate of street canyons in tropical climate. *Building and Environment, 169*, Article 106547.
Napoli, A., Matiu, M., Laiti, L., Barbiero, R., Tombolato, D., Monsorno, S. S., Bellin, A., Zardi, D., & Majone, B. (2026). Building the scientific basis for the adaptation strategy of an Alpine region: The 'State of the climate in Trentino' report. *Climate Services, 41*, Article 100629. https://doi.org/10.1016/j.cliser.2025.100629
Napoli, A., Matiu, M., Laiti, L., Barbiero, R., Bellin, A., Zardi, D., & Majone, B. (2025). Review on climate change impacts on the Water-energy-food-ecosystems (WEFE) Nexus in the North-Eastern Italian Alps. *Climatic Change, 178*, 41. https://doi.org/10.1007/s10584-025-03890-y
Nasrollahi, N., Namazi, Y., & Taleghani, M. (2021). The effect of urban shading and canyon geometry on outdoor thermal comfort in hot climates: A case study of Ahvaz, Iran. *Sustainable Cities and Society, 65*, Article 102638. https://doi.org/10.1016/j.scs.2020.102638
Nasrollahi, N., & Rostami, E. (2023). The impacts of urban canyons morphology on daylight availability and energy consumption of buildings in a hot-summer Mediterranean climate. *Solar Energy (Phoenix, Ariz.), 266*, Article 112181.
Oke, T. R., Mills, G., Christen, A., & Voogt, J. A. (2017). *Urban Climates*. Cambridge: Cambridge University Press. https://doi.org/10.1017/9781139016476
Othman, H. A. S., & Alshboul, A. A. (2020). The role of urban morphology on outdoor thermal comfort: The case of Al-Sharq City – Az Zarqa. *Urban Climate, 34*, 100706. https://doi.org/10.1016/j.uclim.2020.100706
Ouyang, W., Morakinyo, T. E., Ren, C., & Ng, E. (2020). The cooling efficiency of variable greenery coverage ratios in different urban densities: A study in a subtropical

climate. *Building and Environment, 174*, Article 106772. https://doi.org/10.1016/j.buildenv.2020.106772
Ouyang, W., Sinsel, T., Simon, H., Morakinyo, T. E., Liu, H., & Ng, E. (2022). Evaluating the thermal-radiative performance of ENVI-met model for green infrastructure typologies: Experience from a subtropical climate. *Building and Environment, 207*, Article 108427. https://doi.org/10.1016/j.buildenv.2021.108427
Patle, S., & Ghuge, V. V. (2025). Urban form and climate interplay: A meso to micro level assessment in a semi-arid climate city from a thermal comfort perspective. *Sustainable Cities and Society, 134*, Article 106888. https://doi.org/10.1016/j.scs.2025.106888
Perera, N. G. R., & Emmanuel, R. (2018). A "Local Climate Zone" based approach to urban planning in Colombo, Sri Lanka. *Urban Climate, 23*, 188–203. https://doi.org/10.1016/j.uclim.2016.11.006
Pezzuto, C. C., Alchapar, N. L., & Correa, E. N. (2022). Urban cooling technologies potential in high and low buildings densities. *Solar Energy Advances, 2*, Article 100022.
Piazza, A., Panettieri, E., & Tais, M. (2024). *Analisi meteorologica mensile*. Agosto, 2024.
Piselli, C., Castaldo, V. L., Pigliautile, I., Pisello, A. L., & Cotana, F. (2018). Outdoor comfort conditions in urban areas: On citizens' perspective about microclimate mitigation of urban transit areas. *Sustainable Cities and Society, 39*, 16–36. https://doi.org/10.1016/j.scs.2018.02.004
P.Tootkaboni, M., Ballarini, I., Zinzi, M., & Corrado, V. (2021). A comparative analysis of different future weather data for building energy performance simulation. *Climate, 9*. https://doi.org/10.3390/cli9020037
Rafiee, A., Dias, E., & Koomen, E. (2016). Local impact of tree volume on nocturnal urban heat island: A case study in Amsterdam. *Urban Forestry & Urban Greening, 16*, 50–61. https://doi.org/10.1016/j.ufug.2016.01.008
Rahman, M. A., Stratopoulos, L. M. F., Moser-Reischl, A., Zölch, T., Häberle, K. H., Rötzer, T., Pretzsch, H., & Pauleit, S. (2020). Traits of trees for cooling urban heat islands: A meta-analysis. *Building and Environment, 170*, Article 106606. https://doi.org/10.1016/j.buildenv.2019.106606
Richard, Y., Emery, J., Dudek, J., Pergaud, J., Chateau-Smith, C., Zito, S., Rega, M., Vairet, T., Castel, T., & Thévenin, T. (2018). How relevant are local climate zones and urban climate zones for urban climate research? Dijon (France) as a case study. *Urban Climate, 26*, 258–274.
Rydin, Y., Bleahu, A., Davies, M., Dávila, J. D., Friel, S., De Grandis, G., Groce, N., Hallal, P. C., Hamilton, I., & Howden-Chapman, P. (2012). Shaping cities for health: complexity and the planning of urban environments in the 21st century. *The Lancet, 379*, 2079–2108.
Salata, F., Golasi, I., de Lieto Vollaro, R., & de Lieto Vollaro, A. (2016a). Urban microclimate and outdoor thermal comfort. A proper procedure to fit ENVI-met simulation outputs to experimental data. *Sustainable Cities and Society, 26*, 318–343.
Salata, F., Golasi, I., Vollaro, R., de, L., Vollaro, A., & de, L. (2016b). Outdoor thermal comfort in the Mediterranean area. A transversal study in Rome, Italy. *Building and Environment, 96*, 46–61. https://doi.org/10.1016/j.buildenv.2015.11.023
Salehi, A., & Nasrollahi, N. (2024). Assessing vegetation distribution based on geometrical and morphological characteristics of the urban fabric to provide thermal comfort for pedestrians: A case study in Sanandaj. *Sustainable Cities and Society, 104*, Article 105297. https://doi.org/10.1016/j.scs.2024.105297
Scherer, D., Fehrenbach, U., Beha, H.-D., & Parlow, E. (1999). Improved concepts and methods in analysis and evaluation of the urban climate for optimizing urban planning processes. *Atmospheric Environment, 33*, 4185–4193.
Semeraro, T., Gatto, E., De Bellis, L., Luvisi, A., Emmanuel, R., & Buccolieri, R. (2023). A decision-making framework for promoting the optimum design and planning of Nature-based Solutions at local scale. *Urban Forestry & Urban Greening, 84*, Article 127945.
Shi, Y., Lau, K. K.-L., Ren, C., & Ng, E. (2018). Evaluating the local climate zone classification in high-density heterogeneous urban environment using mobile measurement. *Urban Climate, 25*, 167–186. https://doi.org/10.1016/j.uclim.2018.07.001
Shooshtarian, S., Lam, C. K. C., & Kenawy, I. (2020). Outdoor thermal comfort assessment: A review on thermal comfort research in Australia. *Building and Environment, 177*, Article 106917. https://doi.org/10.1016/j.buildenv.2020.106917
Simon, H., Lindén, J., Hoffmann, D., Braun, P., Bruse, M., & Esper, J. (2018). Modeling transpiration and leaf temperature of urban trees–A case study evaluating the microclimate model ENVI-met against measurement data. *Landscape and Urban Planning, 174*, 33–40.
Sola-Caraballo, J., Lopez-Cabeza, V. P., Roa-Fernández, J., Rivera-Gomez, C., & Galan-Marin, C. (2024). Assessing and upgrading urban thermal resilience of a Spanish MoMo neighbourhood over the span of 1960–2080. *Building and environment, 256*, Article 111485. https://doi.org/10.1016/j.buildenv.2024.111485
Song, J., Huang, B., Kim, J. S., Wen, J., & Li, R. (2020). Fine-scale mapping of an evidence-based heat health risk index for high-density cities: Hong Kong as a case study. *Science of the Total Environment, 718*, Article 137226. https://doi.org/10.1016/j.scitotenv.2020.137226
Srivanit, M., & Jareemit, D. (2020). Modeling the influences of layouts of residential townhouses and tree-planting patterns on outdoor thermal comfort in Bangkok suburb. *Journal of Building. Engineering, 30*, Article 101262.
Stead, D., & Meijers, E. (2009). Spatial Planning and Policy Integration: Concepts, Facilitators and Inhibitors. *Planning Theory & Practice, 10*, 317–332. https://doi.org/10.1080/14649350903229752
Stewart, I. D., & Oke, T. R. (2012). Local climate zones for urban temperature studies. *Bulletin of the American Meteorological Society, 93*, 1879–1900. https://doi.org/10.1175/BAMS-D-11-00019.1
Susca, T., Zanghirella, F., & Del Fatto, V. (2023). Building integrated vegetation effect on micro-climate conditions for urban heat island adaptation. Lesson learned from Turin and Rome case studies. *Energy and buildings, 295*, Article 113233.
Tabatabaei, S. S., & Fayaz, R. (2023). The effect of facade materials and coatings on urban heat island mitigation and outdoor thermal comfort in hot semi-arid climate. *Building and Environment, 243*, 110701. https://doi.org/10.1016/j.buildenv.2023.110701
Taleghani, M., & Berardi, U. (2018). The effect of pavement characteristics on pedestrians' thermal comfort in Toronto. *Urban Climate, 24*, 449–459.
Taleghani, M., Kleerekoper, L., Tenpierik, M., van den Dobbelsteen, A., 2015. Outdoor thermal comfort within five different urban forms in the Netherlands. Spec. Issue Clim. Adapt. Cities 83, 65–78. https://doi.org/10.1016/j.buildenv.2014.03.014.
Top, S., Milošević, D., Caluwaerts, S., Hamdi, R., & Savić, S. (2020). Intra-urban differences of outdoor thermal comfort in Ghent on seasonal level and during record-breaking 2019 heat wave. *Building and Environment, 185*, Article 107103.
Tseliou, A., Koletsis, I., Pantavou, K., Thoma, E., Lykoudis, S., & Tsiros, I. (2022). Evaluating the effects of different mitigation strategies on the warm thermal environment of an urban square in Athens, Greece. *Urban Climate, 44*, Article 101217.
Tsoka, S., Zaraveli, Z., Theodoridou, I., & Velikou, K. (2025). Modeling future urban microclimates in Athens, Greece: An ENVI-met analysis of local climate zones under different emission scenarios. *Buildings, 15*, 3986. https://doi.org/10.3390/buildings15213986
Tudoroiu, M., Eccel, E., Gioli, B., Gianelle, D., Schume, H., Genesio, L., & Miglietta, F. (2016). Negative elevation-dependent warming trend in the Eastern Alps. *Environmental Research Letters : ERL [Web site], 11*, Article 044021.
UN Habitat. (2022). World cities report 2022. envisaging the future of cities (No. HS/004/22E). In *United Nations Human Settlements Programme (UN-Habitat)*.
Verdonck, M. L., Demuzere, M., Hooyberghs, H., Beck, C., Cyrys, J., Schneider, A., Dewulf, R., & Van Coillie, F. (2018). The potential of local climate zones maps as a heat stress assessment tool, supported by simulated air temperature data. *Landscape and Urban Planning, 178*, 183–197.
Wang, Y., Guo, Z., & Han, J. (2021). The relationship between urban heat island and air pollutants and them with influencing factors in the Yangtze River Delta, China. *Ecological Indicators, 129*, Article 107976. https://doi.org/10.1016/j.ecolind.2021.107976
Wong, N. H., Tan, C. L., Kolokotsa, D. D., & Takebayashi, H. (2021). Greenery as a mitigation and adaptation strategy to urban heat. *Nature Reviews Earth & Environment, 2*, 166–181.
Wu, Y., Patuano, A., Mashhoodi, B., Lenzholzer, S., Acred, A., & Zertuche, L. N. (2025). How small green spaces cool urban neighbourhoods: Optimising distribution, size and shape. *Landscape and Urban Planning, 253*, Article 105224. https://doi.org/10.1016/j.landurbplan.2024.105224
Yan, S., Zhang, T., Wu, Y., Lv, C., Qi, F., Chen, Y., Wu, X., & Shen, Y. (2023). Cooling effect of trees with different attributes and layouts on the surface heat island of urban street canyons in summer. *Atmosphere, 14*. https://doi.org/10.3390/atmos14050857
(Cecilia) Yang, J., Jin, S., Xiao, X., Jin, C., Xia, J., Li, X., & Wang, S. (2019). Local climate zone ventilation and urban land surface temperatures: Towards a performance-based and wind-sensitive planning proposal in megacities. *Sustainable Cities and Society, 47*, Article 101487. https://doi.org/10.1016/j.scs.2019.101487.
Zaerpour, M., Papalexiou, S. M., & Pietroniro, A. (2025). Increasing tree canopy lowers urban air temperature by up to 1.5°C in heat-prone areas. *npj Urban Sustainability, 5*, 92. https://doi.org/10.1038/s42949-025-00277-x
Zhang, H., Bai, J., Zhao, J., Guo, F., Zhu, P., Dong, J., & Cai, J. (2024). Application and future of local climate zone system in urban climate assessment and planning—bibliometrics and meta-analysis. *Cities (London, England), 150*, Article 104999. https://doi.org/10.1016/j.cities.2024.104999
Zhao, Q., Sailor, D. J., & Wentz, E. A. (2018). Impact of tree locations and arrangements on outdoor microclimates and human thermal comfort in an urban residential environment. *Urban Forestry & Urban Greening, 32*, 81–91.
Zölch, T., Maderspacher, J., Wamsler, C., & Pauleit, S. (2016). Using green infrastructure for urban climate-proofing: An evaluation of heat mitigation measures at the micro-scale. *Urban Forestry & Urban Greening, 20*, 305–316.